FM2001

Deep Structure of the Shelf and Slope of the Northern Gulf of Mexico

Part A: Expanding Spread Profile (ESP) Experiments

by

Joseph D. Phillips and Donald F. Dean

Final Technical Report

December 1986

Institute for Geophysics
The University of Texas at Austin
4920 North I.H. 35
Austin, Texas 78751

University of Texas, Institute for Geophysics Technical Report No. 46

Deep Structure of the Shelf and Slope of the Northern Gulf of Mexico

Part A: Expanding Spread Profile Experiments

ABSTRACT

Four, two-ship expanding spread profiles (ESP's), each 80 km long, were collected along a transect near 94°W longitude extending from the Texas shelf edge to the Sigsbee abyssal plain. The purpose of the work was to determine the deep sediment, basement and sub-basement velocity structure beneath regions masked by salt deposits. ESP's 2 and 3, located along the shelf and upper slope, were sited to avoid the shallower massive salt diapiric structures. ESP 4 was positioned over relatively flat-lying, layered salt deposits on the lower slope. ESP 5 was located just beyond the Sigsbee Escarpment on the abyssal plain.

The profiles were acquired at 300 meters shot distance intervals using two, 2000 in^3/2000 psi airguns with Miniranger and LORAN-C navigation and were recorded with 24 and 48 trace multichannel streamer arrays having 50 and 70 meter hydrophone group intervals, respectively. This configuration provided overlapping data trace coverage which was sorted into 50 meter offset "bins" and summed. Offset range-travel time (X-T) plots have been constructed.

Ray-tracing and direct Tau-P velocity inversion of the slant-stacked, wide-angle reflection and refraction arrivals suggests that a 5.0 to 6.0 km/sec basement exists beneath the sediments (2.0-4.4 km/sec) along the shelf edge (ESP 2) and upper slope (ESP 3). Beneath the lower slope (ESP 4) a thin salt layer (~1-2 km thick) with velocity of 4.0 km/sec appears to be underlain by sedimentary strata (3.8-4.8 km/sec) resting on oceanic type crust having layer velocities of 6.9-7.5 km/sec. A low-velocity layer may be present directly beneath the salt. ESP 5, on the Sigsbee rise shows a thick sedimentary section overlying oceanic type crust with 6.0 km/sec and 6.9 km/sec velocity layers and underlain by Moho with a 8.1 km/sec velocity.

INTRODUCTION

The continental margin off Texas and Louisiana is marked by very thick sediments and salt diapirs deposited since late Jurassic time as Yucatan rifted away from North America to form the Gulf of Mexico (Buffler, et al., 1978). These deposits, which probably exceed 15 km thickness in many places have masked the underlying pre- and syn-rift crustal rocks from detailed examination using conventional seismic reflection and refraction methods (Antoine and Ewing, 1963; Ewing et al., 1960). Accordingly, the University of Texas Institute for Geophysics (UTIG) and the United States Geological Survey (USGS) proposed to study the deep crustal structure by employing two advanced seismic techniques; namely, wide-angle two-ship multichannel seismic (MCS) arrays and ocean bottom seismometers (OBS). We hoped to attain a higher signal to noise ratio than experiments heretofore by combining a high energy, uniform signature airgun sound source with (1) the noise rejection afforded by multichannel streamer signal stacking methods and (2) by recording on the quiet seafloor environment with ocean bottom seismometers, respectively. The airgun sources also offer the advantage of being more accurately timed and can be fired at a much closer interval along the ship track than the explosive sources used in earlier wide angle experiments. Such high spatial data density allows modern digital computer signal enhancement and analysis techniques to be used in the processing of seismic data. The efficacy of computer techniques for large aperture seismic research cannot be overstated.

The field study utilizing these advanced seismic techniques for the first time in the northern Gulf of Mexico, was conducted during the late fall of 1983 (Figure 1). It was a two-phase study supported by several U.S. oil companies. Part A was a two-ship experiment done in November 1983, using the R.V. Moore (Cruise FM 20-01) of the University of Texas and the R.V. Gyre (Cruise 83-14) chartered by the USGS from Texas A&M University. It was designed to collect four (4) multichannel expanding spread profiles (ESP) and a continuous, wide aperture constant offset profile (COP) using the techniques described by Stoffa and Buhl (1979). The profiles were shot along a transect extending from the deep ocean basin

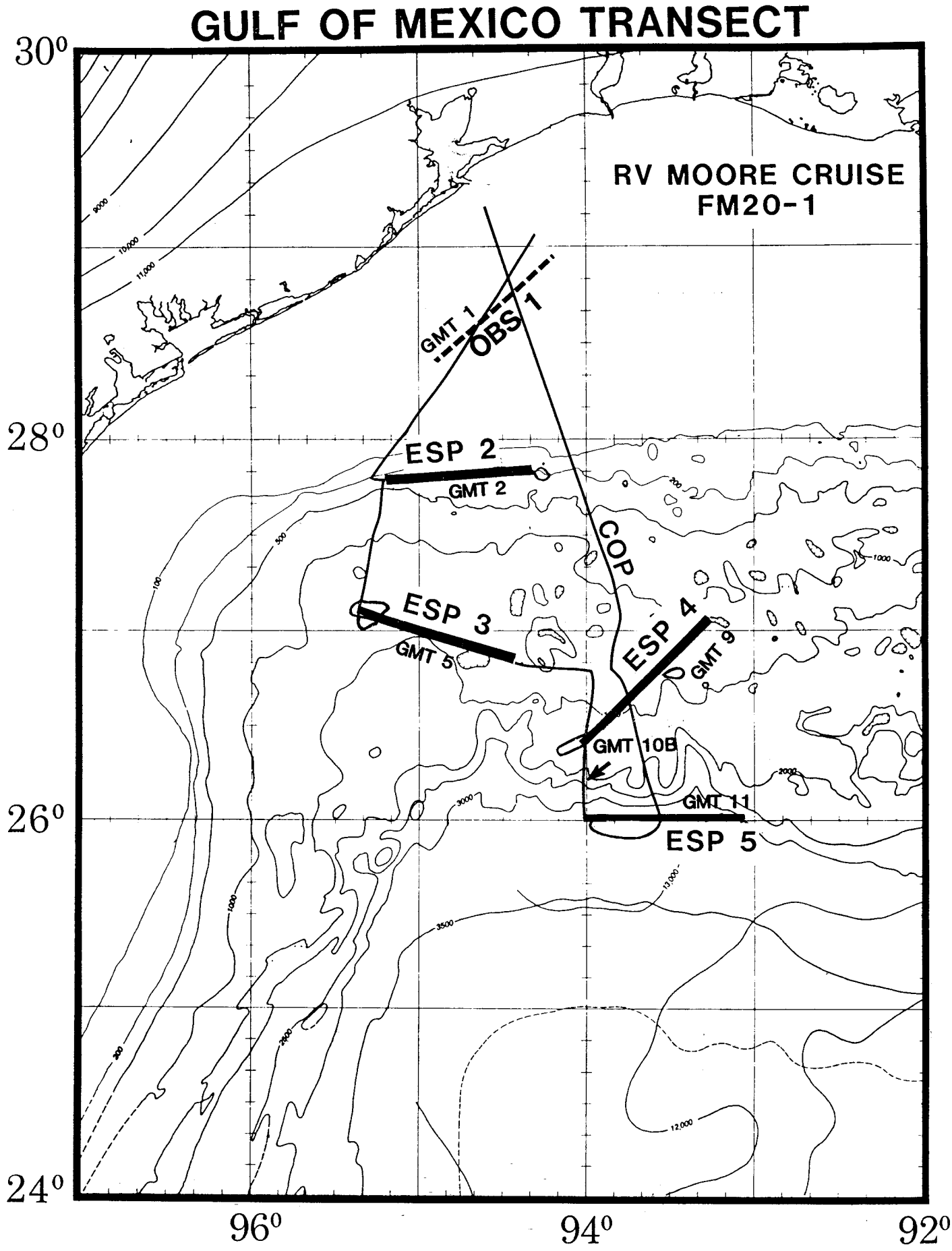

FIGURE 1. Map of northwest Gulf of Mexico showing the location of ESP 2-5 and MCS reshoot lines (GMT-2,GMT-5,GMT-9,GMT-11). Also shown is the location of OBS Line 1 (dashed line) and MCS tieline GMT-10B.

northward across the continental margin to near Galveston (Figure 1). Unfortunately, high sea conditions during the experiment caused extreme streamer hydrophone noise which prevented the accomplishment of the latter COP objective. Conventional multichannel seismic (MCS) lines and sonobuoy stations were also shot along each of the ESP lines and selected tie lines between the ESP profiles. The detailed location and shooting/receiving ship configuration for all lines are listed in Appendix Tables A, B and C.

Part B was an ocean bottom seismometer (OBS) experiment done in December 1983 with only the R.V. Moore (Cruise FM 20-02) but using the same airgun sound source used in the ESP experiments. The OBS lines were located precisely along the same lines shot during the previous ESP work. This report describes only the results of the Part A Expanding Spreading Profile Experiments and associated MCS lines.

FIELD EXPERIMENT

The four multichannel, expanding spread profile lines (ESP2-5) were located by UTIG scientists in consultation with the oil company sponsors (Figure 1). The primary objective in positioning these lines was to avoid shallow salt structures as much as possible in order to minimize attenuation and scattering effects. ESP, OBS and MCS data were collected along each of these lines. A fifth line (OBS1), not planned for ESP experiments, was previously positioned solely for the OBS studies and is shown by a dashed line in Figure 1. Unfortunately, the MCS line subsequently shot along this line (see Part B) showed its southwestern end crossed over a massive salt structure.

Figure 2 shows the ray path geometry for acquiring the field data along the expanding spread profiles (ESP 2-5). In these experiments, the shooting and receiving ships first pass abeam of each other at about 1 nm range near a predetermined mid-point. Each ship then steams away from the mid-point at the same speed, approximately 5 knots (9 km/hr), out to a range of about 50 kms. Since the effective ship separation rate is 10 knots (18 km/hr), a 60 second air gun firing rate provides a nominal 300 meters shot distance interval. This constant separation rate arrangement results in all the reflection mid-points between each shot and the hydrophone streamer being fixed on the seafloor within a distance equal to about half the receiving ship's streamer length. Note that this ESP shot-receiver ray path geometry is analogous to the configuration used to gather conventional MCS data into individual common depth point (CDP) bins along a ship's track. That is, in the CDP method those shot-receiver pairs which have the same reflection point or more accurately, common mid-point (CMP) along the ship's track are sorted (gathered) into a common bin. In fact, an ESP experiment could be considered to be a single, "mega-CDP" bin gather.

The ships' end point positions for each ESP and the calculated average mid-point are shown in Appendix Table A. Figures 3A and B show the respective ship's tracks as the ships passed each other near the mid-points. The calculated shot distance interval and ships' offset range as the ships traversed along each ESP line are shown in Figures 4A and B and 5A and B,

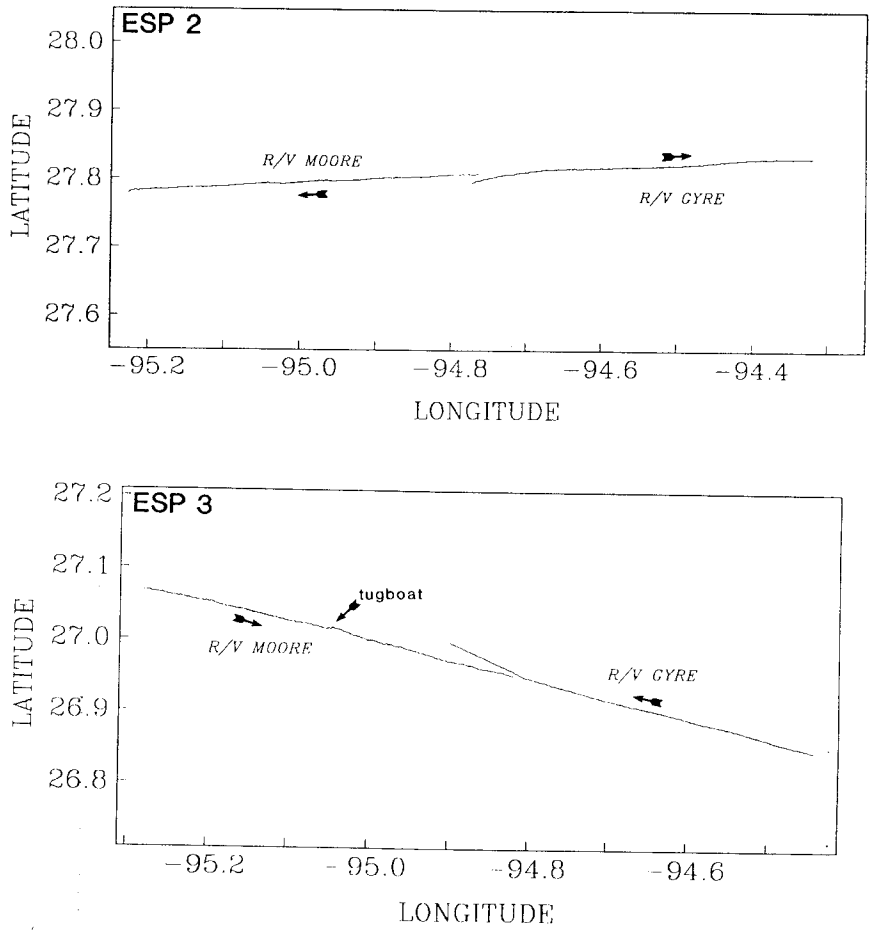

FIGURE 3a. Track chart showing location and traverse direction of each ship. R/V Moore was the shooting ship and R/V Gyre was the receiving ship for ESP 2 and ESP 3.

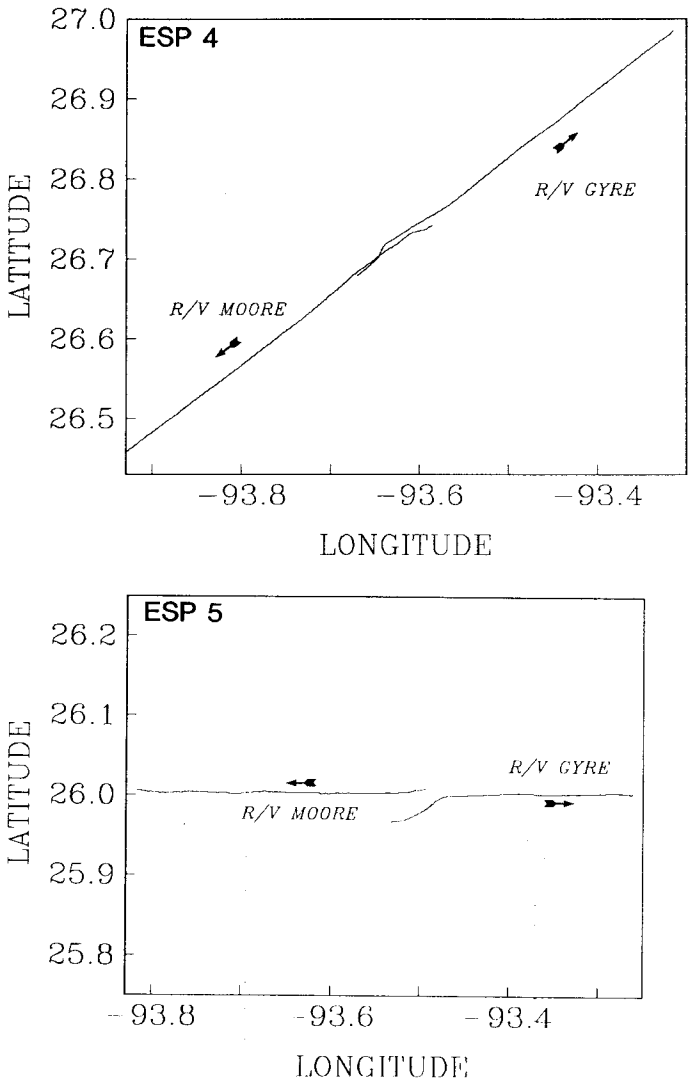

FIGURE 3b. Track chart showing location and traverse direction of each ship. R/V Gyre was the shooting ship and R/V Moore was the receiving ship for ESP 4 and ESP 5.

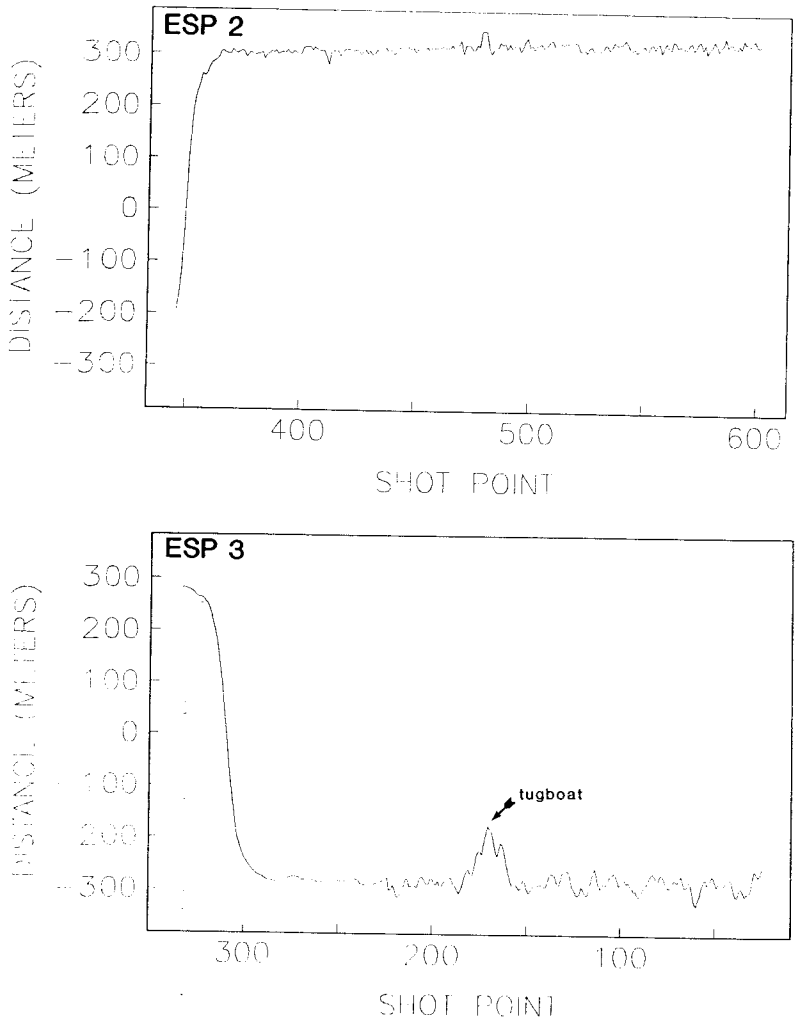

FIGURE 4a. Shot distance interval for ESP 2 and ESP 3.

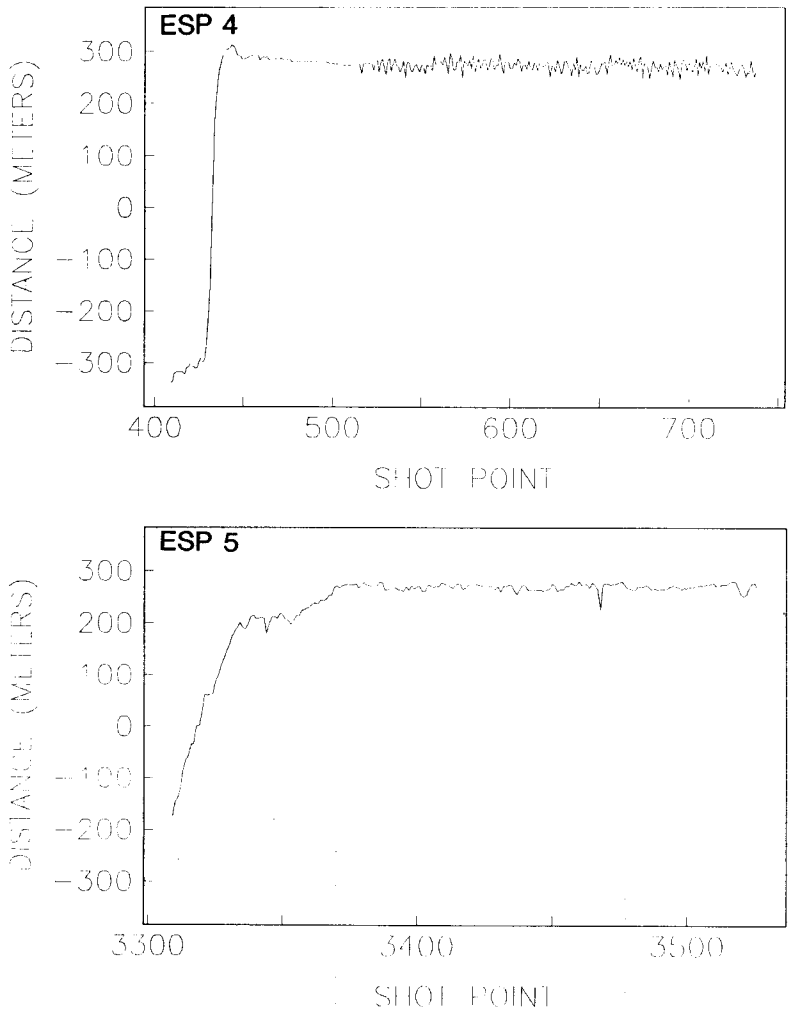

FIGURE 4b. Shot distance interval for ESP 4 and ESP 5.

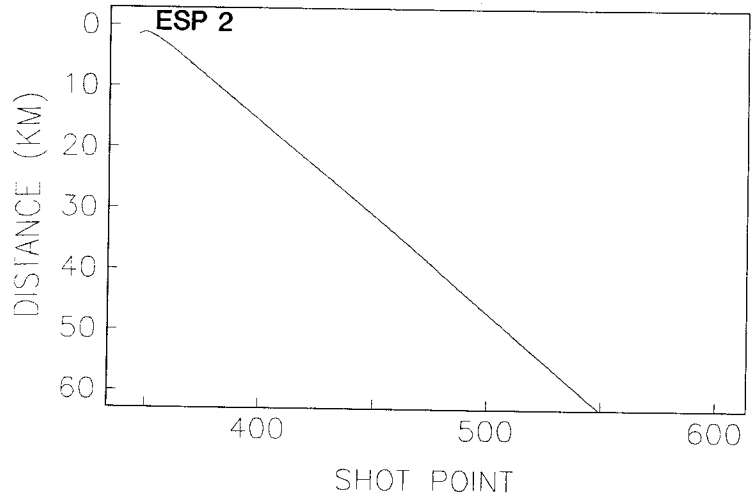

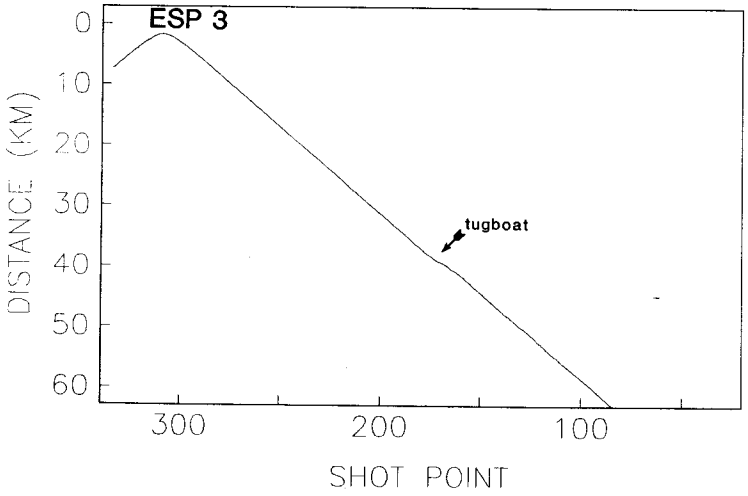

FIGURE 5a. Offset ranges for ESP 2 and ESP 3.

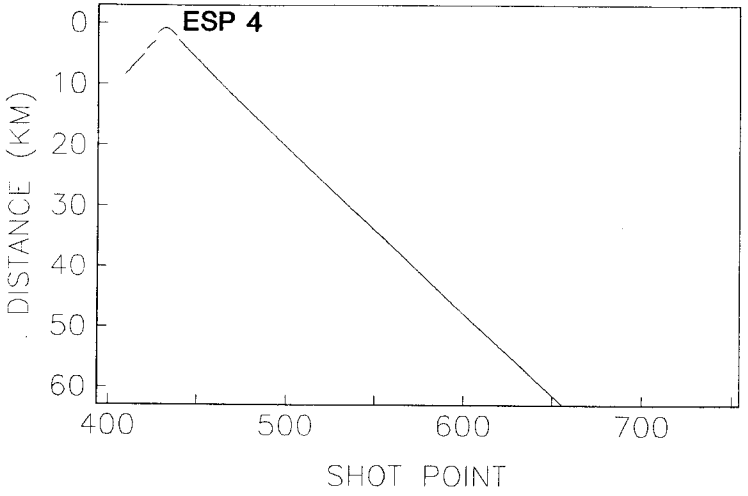

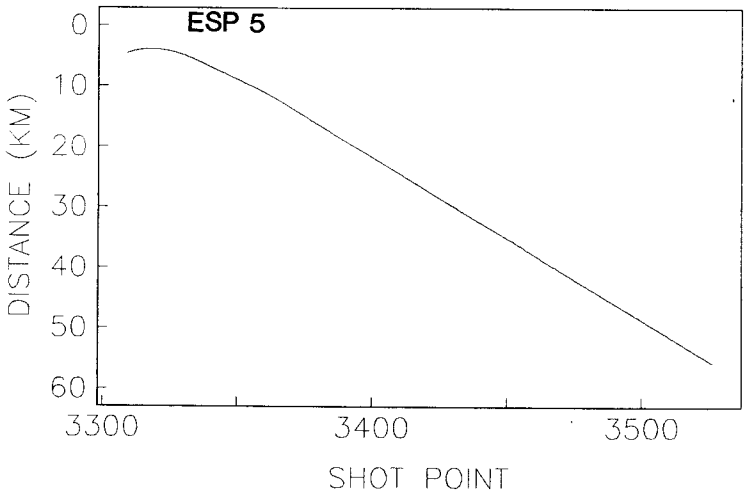

FIGURE 5b. Offset ranges for ESP 4 and ESP 5.

respectively. A plot of the geographic mid-points between the ships' radio navigation attennae calculated from the Loran-C positions at successive shot times along each ESP are shown in Figures 6A and B. The tight grouping of the mid-points, the small changes in shot distance interval and the smooth linear variation of the ships' offset attests to the overall close speed and course control of the ships during the experiment. Only during ESP 3, when a tow boat and barge crossed the receiving ship's path (MOORE), was there significant mid-point scatter or sharp shot distance and offset changes. AGC sonobuoys were also deployed and digitally recorded by the MOORE along each ESP line as well as the OBS lines shot later during Cruise FM20-02. The sonobuoy station locations are summarized in Appendixes Tables B and C, respectively. However, no results from the sonobuoy observations are included in this report.

Instrumentation:

Air Gun Sources

Both the MOORE and GYRE were equipped with similar airgun source arrays. These consisted of two, Bolt Model 800 C, 2000 cu. in. airguns operating at 2000 psi pressure. During the ESP experiment the shooting ships traveled at 5.0 knots nominal speed and fired their airgun arrays at a 60 second repetition rate. This provided a shot distance interval of about 150 m and shot receiver distance interval of 300 m. For the conventional MCS lines, the MOORE firing repetition rate was 30 seconds. However, the GYRE fired its airguns at a fixed shot distance interval of 50 meters (approximately 20 seconds repetition rate). The MCS lines which were acquired simultaneously during an ESP experiment were shot at a 60 second repetition rate, resulting in a nominal 150 m shot distance interval.

Hydrophone Streamer Receiving Arrays

The hydrophone streamer arrays for the ships were markedly different. The MOORE streamer had 48 active receiving sections, each 30 meters long and separated by 40 meter inactive, dead sections. This provided an effective group interval length of 70 meters with a total streamer length of 3290 meters. The streamer was fitted with fixed depth controller

"birds" which were pre-set to tow at about 13 meters depth in calm seas. The GYRE streamer had 24 active receiving sections each 50 meters long, providing a group interval length of 50 meters and a total streamer length of 1200 meters. This streamer was fitted with controllable depth "birds" and which could maintain a towing depth of about 13 meters in moderate sea states. Significantly, the streamer's depth could be depressed to as much as 50 meters during high sea states.

Timing Control and Data Logging

Absolute timing control for the two ships was provided by identical GOES satellite time signal receivers (True-Time Systems). Each ship's laboratory was also equipped with precision, crystal oscillator (Hewlett Packard/MOORE) and Cesium (FTS/GYRE) clocks for controlling its internal gun firing and navigation data recording sequence and to give redundancy to the satellite timing system. These laboratory clocks provided precise time to within 1 part in 10^9 and 10^{14}, respectively. The primary time and navigation data logging systems aboard each ship were also identical. Hewlett Packard series H/P 1000 computer-based, magnetic tape logging systems were kindly provided by one of the oil company sponsors. These systems recorded the shot time, data record time breaks, inter-ship MINIRANGER radar distance, TRANSIT satellite and LORAN-C geographic position information and shot number. The logging systems were also linked by a UHF radio which would allow the master ship (MOORE) to control the airgun firing and data recording of both ships. However, this command and control aspect of the H/P logging system was not used in these experiments. Additional independent data logging systems were also used aboard both ships to provide redundant recording of the navigational and timing information. The MOORE logger was a PDP-11/03 computer based system. A Western Geophysical integrated navigation system (WINS) logged these data aboard the GYRE.

Navigation

LORAN-C was the primary navigational control for the experiments. Both ships were equipped with identical NORTHSTAR model 6000 and INTERNAV model LC 404 receivers. The NORTHSTAR provided automatic conversion of geographic position and ships speed information. This allowed precision real time control of the ships' paths and speed which was critical for maintaining the constant mid-point geometry during the ESP experiments. The INTERNAV unit was a higher resolution receiver than the NORTHSTAR, providing +0.01 micro sec delay data and was used in the post-cruise processing. Overall, the LORAN-C positional accuracy was judged to be on the order of 10 to 20 meters. The inter-ship range between ships was measured with identical MOTOROLA MINIRANGER radar ranging systems installed on each ship. Each ship had a slave and master unit. These systems provide redundant range information accurate to within 5 meters out to line of sight ranges of about 20 kms.

Seismic Data Acquisition and Recording

The seismic data recording systems aboard each ship were somewhat different. The MOORE'S system consisted of a Texas Instrument DFS IV data acquisition system linked to a Digital Equipment Corporation (DEC) PDP 11/34-based computer which received the raw, multiplexed, time sequential data and converted it to demultiplexed trace-sequential data. This "demux" data was written to magnetic tape after each shot in SEG-D demultiplexed exchange format. The GYRE seismic data was collected with a DFS V system in SEG B, multiplexed time sequential format and was later demultiplexed at the USGS processing center in Denver, Colorado.

Field Parameters:

The various equipment and operational parameters for each of the ships deployed for the ESP and MCS work are listed below:

TABLE 1
Gulf of Mexico Transect Project Field Parameters

MOORE

Source: Two Airguns, Bolt model 800C, 2000 in^3 (33 L each) fired at 2000 psi ($1.36 \times 10^7 NT/m^2$)

Towing depth: 35 feet (11 m)

Firing Repetition rate: 30 sec (MCS), 60 sec (ESP)

Ship speed: 5 knots (9 km/hr) nominal

Shot spacing interval: 70m (MCS), 140 m (ESP), both nominal

Hydrophone streamer: Western Geophysical, 48 channel, 70 meter Group Interval (30 meters active and 40 meter dead sections). Total active streamer length 3290 meter.

Airgun source to near receiver channel offset: 190 meters.

Recording System: DFS IV with PDP-11/34 (DEMUX) (Seismics), Gulf HP logger and PDP-11/03

Record Length Interval: 15 second (MCS), 40 sec (ESP), no delays

Sample Interval: 4 ms

DFS IV filter pass band: 3-62 hz (72 db/octave roll-off)

GYRE

Source: Same as MOORE

Towing Depth: Same as MOORE

Firing Repetition rate: 20 seconds nominal to maintain precise 50 meter shot distance interval (MCS), 60 seconds (ESP)

Ship speed: Same as MOORE

Shot spacing: 50 meters (MCS), 150 meters nominal (ESP)

Hydrophone streamer: Teledyne, 24 channel 50 meter group interval (50 meter active section). Total active streamer length: 1150 meters.

Airgun source to near receiver channel offset: 100 meters.

Recording Systems: DFS V (Seismics), Gulf HP Logger and USGS/WINS.

Recording Length: 12 seconds (MCS), 40 sec (ESP), no delays

Sample Interval: 4 ms.

DFS V filter passband: 6-64 hz (72 db/octave roll-off)

Field Operations:

The two-ship field survey work was carried out during the period 13-20 November 1983 aboard R. V. MOORE (cruise 20-01) and R. V. GYRE (cruise 83-14). It was planned that the MOORE with its longer, 48 channel streamer would be the receiving ship for all the ESP experiments and that both ships would shoot and receive for the COP transect line. Unfortunately, during the study three (3) cold front weather systems passed over the survey area which interrupted this shooting/receiving ship plan. The first two of these fronts, accompanied by high winds and seas (greater than 40 knots/~15 feet), caused the MOORE's preset, fixed depth streamer to be extremely noisy on several occasions. It could not be depressed below the storm wave base. This caused delays and necessitated that the GYRE with its controllable depth streamer become the receiving ship for ESP 2 and ESP 3 (Figure 1). Although this arrangement proved satisfactory, the greatly improved signal to noise ratio that was expected from use of the MOORE's 48 channel streamer was not realized. However, an adequate S/N ratio appears to have been attained to provide deep pentration at the ESP sites. Finally, a third frontal passage on 18/19 November at the very beginning of the COP transect line, where both ships had to receive, caused both ship's streamers to become extremely noisy. This forced the abandonment of the COP experiment after only 6 hours. No useful wide aperture, two-ship seismic data were collected.

DATA PROCESSING

The single ship, multichannel seismic (MCS) lines acquired aboard R. V. MOORE and R. V. GYRE were processed separately by scientists at UTIG and USGS (Denver), respectively. All two-ship data processing, except for USGS's demultiplexing of the GYRE field tapes, was performed by UTIG scientists. Nearly identical Digital Equipment Corporation VAX 11-780 computers with DISCO* interactive seismic data processing software systems were available at both UTIG and USGS (Denver). These systems were used for all seismic data processing.

Multichannel Seismics (MCS):

Standard common depth point (CDP) seismic reflection processing techniques were used to analyse and stack both MOORE's and GYRE's single ship MCS data. The general processing sequence is shown in Table 2. The primary difference in the processing of the MOORE and GYRE data was the method for determining the shot distance intervals along each profile line. For GYRE the data were actually collected at sea by firing (shooting) the airguns at a constant, elapsed shot distance of 50 meters. The interval distance traveled was calculated in real time from smoothed LORAN-C navigational data. For the MOORE the airguns were fired at a fixed time interval of 30 seconds with the ship traveling at a constant speed. The average shot distance interval was calculated later by dividing the seismic line length by the number of shots fired. Since MOORE's speed was nominally held constant at about 5.0 knots, this resulted in a MOORE average shot distance interval of about 70 meters, compared to GYRE's fixed interval of 50 meters.

The CDP binning intervals for the MOORE and GYRE data were 70 meters and 50 meters respectively, which matched the shot and hydrophone group interval distance of each ship. This resulted in nominal 24-fold and 12-fold data trace multiplicity for each MOORE and GYRE bin, respectively, since the streamers' hydrophone group intervals were equal to the shot distance. However, the actual fold along each line varied and was generally less than

*Trademark Digicon Corporation, Houston, Texas.

TABLE 2
Multichannel Seismic (MCS) Data Processing Sequence

	MOORE	GYRE
Step 1)	Field Data Acquisition: SEG-D Demultiplexed Trace-Sequential Format	Field Data Acquisition: SEG-B Multiplexed Time-Sequential Format
Step 2)	Convert Field Data Tapes to Internal VAX/DISCO Format Trace	Demultiplex Field Data Tapes to Internal VAX/DISCO Trace-Sequential Format
3)	Edit shot number/time and digital record number errors	
4)	Eliminate noisy/dead streamer data channels	
5)	Calculate MOORE average shot distance interval (GYRE shots were at fixed 50 meter distance intervals along line)	
6)	Calculate each shot-receiver pair reflection mid-point location and the common mid-point locations (bin) along line	
7)	Sort the data traces for each shot-receiver-pair into nearest common depth point (CDP) or mid-point (CMP) bin according to their offset	
8)	Constant velocity analysis (CVA) of selected CDP bin gathers along line	
9)	Perform normal moveout (NMO) of all CDP gathers along line using CVA results	
10)	Stack NMO-CDP gathers	
11)	Perform deconvolution, bandpass filtering, migration, time/depth conversion and other post-stack CDP processing	
12)	Display/archive final, stacked CDP profile section	

nominal due to the elimination during the data trace editing process of dead and noisy streamer channels caused by high seas.

Expanding Spread Profile (ESP) processing:

An ESP experiment results in a complete suite of shot-receiver offset pairs with ray path geometry that is the equivalent to the ray path geometry that is obtained by the CDP sorting method in gathering conventional multichannel seismic data into a single CDP bin (Figure 2). That is, an ESP contains data traces that were recorded for shot-receiver pairs that had the same seafloor locus of reflection or common mid-point (CMP). However, an ESP differs from a single ship CDP bin gather in that the source-receiver offsets are not at fixed increments based on the physical hydrophone group interval distance. The offset distances vary as the ships change range as they traverse along the seismic line. Also, the maximum offset of an ESP gather is not limited to a distance defined by the streamer's physical length. Despite these important differences the initial processing of the ESP data shown in Table 3 was the same sequence as usual for MCS processing (Table 2) down to step 5. However, beginning with step 6 the following processing was employed.

Synchronization of Shot and Record Time Breaks

Both ships received the same absolute time signals broadcast by the GOES satellite system. This signal, which is received continuously, was used to synchronize each ship's laboratory clock system at the beginning of the experiment to the nearest millisecond. During the experiment both the satellite and the laboratory clock times for the shot and the data record time break were recorded aboard each ship. Post-experiment comparison of the shot and data record times for each ship's satellite and laboratory clock showed very small drift rates during the experiment, generally less than 1.0 millisecond per day. Also the GYRE laboratory clock recorded time breaks were found to be advanced approximately 200-700 milliseconds ahead of the MOORE time breaks relative to the fixed one minute shot/record cycle command time for ESP 3, 4, 5. ESP 2 showed the GYRE offset was approximately 600 milliseconds after

TABLE 3

Expanding Spread Profile (ESP) Data Processing Sequence

STEPS 1-5 Same As MCS Data Processing (Table 2)

STEP 6) Shot Statics:
Correct for clock differences between data recording/shooting systems of each ship

7) Navigation Processing:
Check for Miniranger and LORAN-C signal dropout and noise
Calculate source and receiver offset geometry from Miniranger/LORAN-C information and direct water wave acoustic traveltime

8) Header Edit:
Put offset and shot statics information into trace headers

9) Display shot gathers:
Water bottom reflection arrivals corrected for normal moveout (NMO) at 1500 m/sec water velocity

10) Header Edit:
Trace statics applied to make water bottom reflection arrivals horizontal (flat) to account for streamer curvature

11) Offset Bin Sorting:
All traces within $\pm$25 meters offset distance along profile gathered into 50 meter interval offset bins

12) Header Edit:
Apply a reduction velocity static to align traces within each bin using an 8.0 km/sec phase velocity to enhance deep sub-crustal reflection arrivals

13) Display Bin Gathers:
Final data edit to check horizontal arrival alignment after all offset information and static corrections applied

14) Sum all traces in each bin into single trace positioned at bin center's offset distance

15) Display/Archive final offset-trace (X-T) travel time data set

16) Slant stacking of X-T bin summed data set:
Transformation of X-T domain data to Tau-P domain (intercept time-ray parameter) data set

17) Direct velocity inversion of Tau-P domain data set:
Critical path for maximum coherence graphically interpreted and integrated over appropriate ray parameters to provide velocity-depth function

MOORE. Accordingly, appropriate static corrections were applied to each data record to account for each ship`s clock drift and data acquistion system time delay offset.

Calculation of the source-receiver offset

Since the ESP experimental data set can be regarded as a single, common depth point (CDP) or more accurately, common mid-point (CMP) gather of a large number of source-receiver offset ranges, ESP data can be best analysed if the data traces for each source-receiver pair are first sorted in order of increasing offset. The individual data traces are then gathered according to offset into their nearest offset bins which were arbitrarily located at 50 meter intervals along the profile line. The several traces in each bin are then summed into a single trace to provide a uniform 50 meter interval data trace spacing for the entire ESP profile. With a shot distance of 300 meters the MOORE's 48 channel streamer yielded a nominal data trace redundancy in each bin of 800% (8-fold). The GYRE's 24 channel streamer provided 4-fold redundancy.

Determination of the far offset distances for source-receiver ranges much greater than the streamers' length can be done simply by measuring the distance (range) between the shooting and receiving ship's radio navigation antennae and accounting for the correction that must be made for the distance between the airgun array and each hydrophone channel from the respective ships' attennae. However, when the ships pass each other at close range, generally less than 5 km, the aspect of the streamer's hydrophone channels relative to the ships' tracks must be considered since the airgun source is not co-linear with the streamer. Also, corrections for the curvature of the streamer may be important if the ships are maneuvering as they pass in order to get on line.

Accordingly three distance measurement techniques are necessary to determine the source-receiver offset over the full separation range of the ESP experiments.

1) Far Offsets

LORAN-C radio navigation was used for the ranges beyond the line of sight between ships (greater than about 20 km). For these range determinations, the smoothed LORAN-C

time delays, as measured with the LC404 system, were transformed to geographic coordinates for each ship and the inter-ship distance was calculated. Since the shooting ship's source and the receiving ship's streamer are essentially in a co-linear, end-fire configuration, the offset range for each shot hydrophone receiver channel pair was calculated by accounting for the distance between the ships' radio antennae and their airguns and streamer hydrophone channels. The precision of the LORAN-C derived range measurement is estimated to be about 10-20 meters.

2) Near Offsets

For the closer ranges where the ships are passing near the mid-point, the determination of range for each shot-receiver pair is more complicated due to the fact that the shooting ship's airgun is firing broadside to the length of the receiving ship's streamer. The simple distance measurement between the ships' radio navigation antennae does not allow the precise range (offset) between the shot and each hydrophone receiver channel to be calculated. Although the approximate range can be estimated using the LORAN-C and MINIRANGER navigated ship tracks and the assumption that the streamer trails straight along the ship's track, the true precise range is best calculated by measuring the direct water wave acoustic travel time to each receiver channel and multiplying by the velocity of sound in sea water (1500 m/sec). For example, plots of the direct wave arrivals along the streamer's length as the ships passed near the ESP-5 mid-point (Figure 7a) allow easy calculation of the acoustic range near the closest point of approach (CPA). These horizontal acoustic ranges can be verified by noting the MINIRANGER distance between the ships' antennae and the air gun and hydrophone channel offset distances from their respective antennae for each shot. These acoustic range calculations can also be verified by observing the water bottom reflection arrival wavetrain across the streamers' length before (Figure 7b) and after normal moveout (NMO) correction for the acoustic range (Figure 7c) using the sound velocity of sea water (1500 m/sec). Where the seafloor is flat, the water bottom arrival water train should also be flat (isochronous) with a two-way travel time equal to the normal incidence water depth travel times. The residual dip

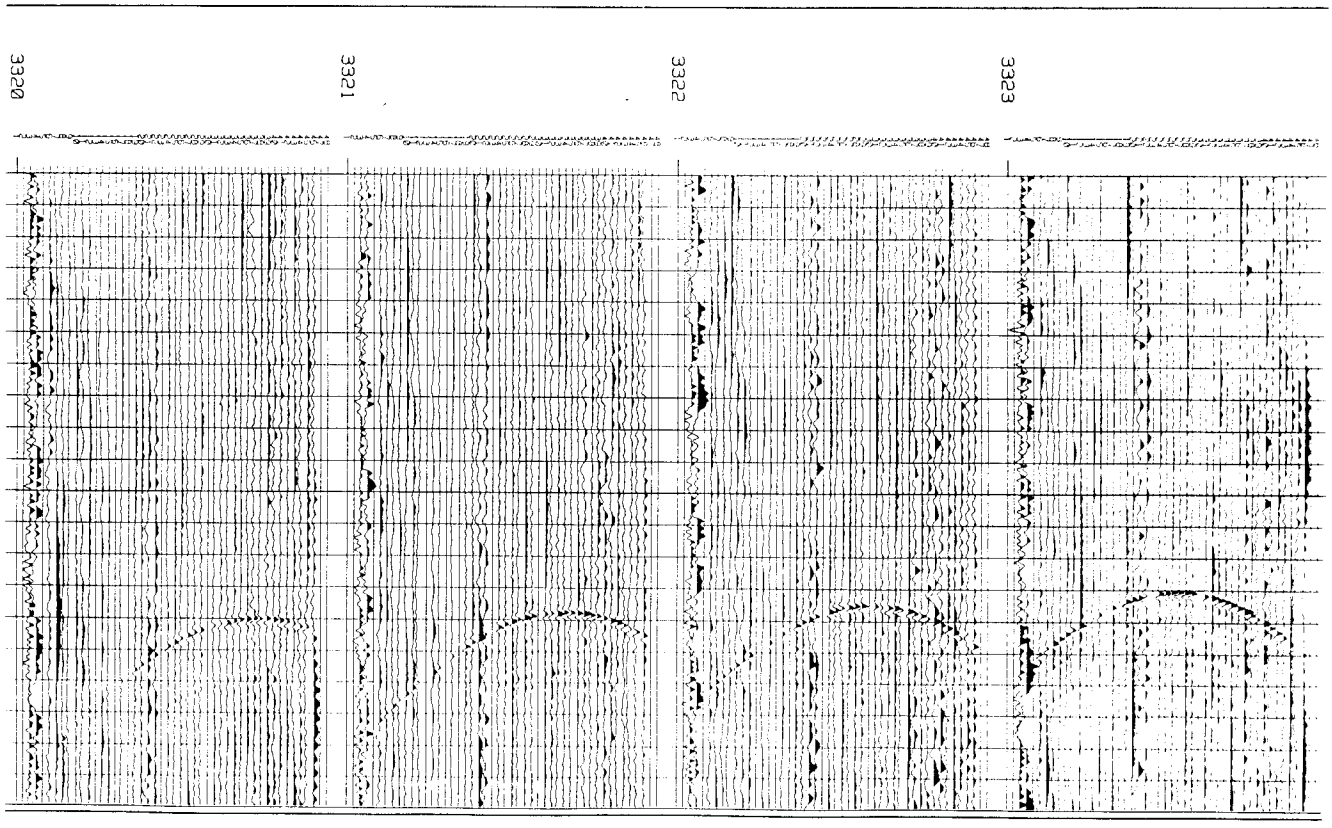

FIGURE 7a. Direct water wave arrivals across Moore's 48 channel hydrophone streamer for succesive airgun shots as Moore and Gyre pass near ESP 5 midpoint.

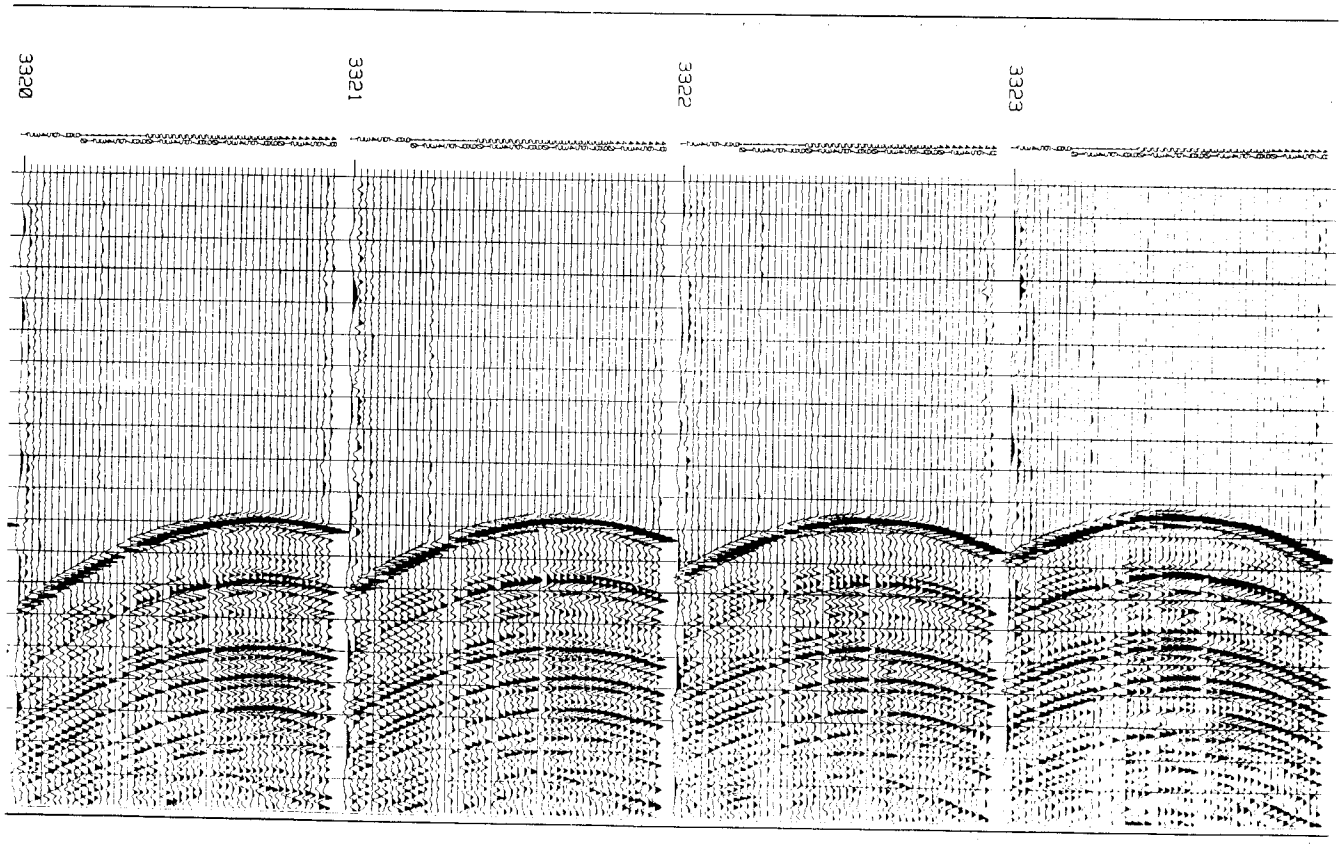

FIGURE 7b. Water bottom reflection arrivals for same shots displayed in Figure 7a.

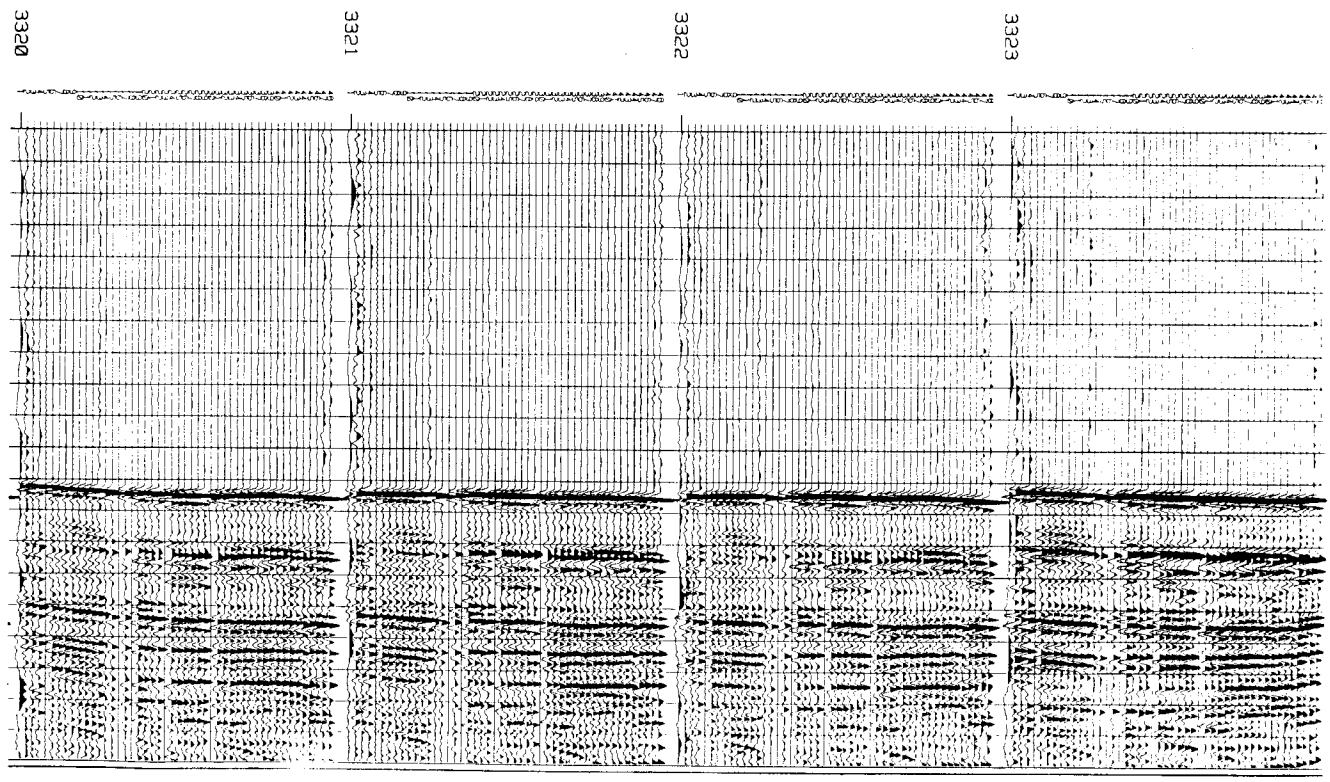

FIGURE 7c. Water bottom reflection arrivals after applying normal moveout correction for offset ranges derived from direct water wave travel times shown in Figure 7a. Note slight dip of arrival toward head of streamer (right, channel 48).

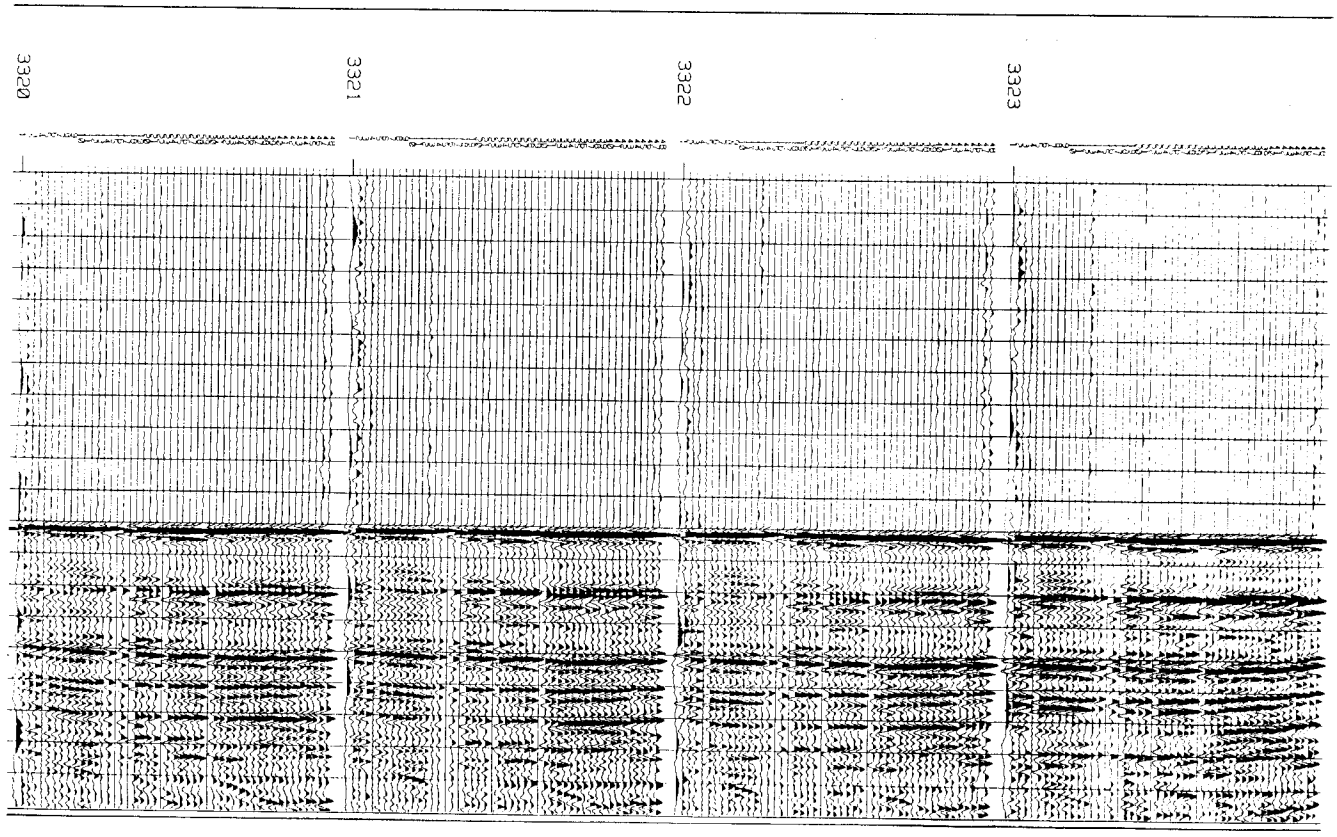

FIGURE 7d. Water bottom reflection arrival after applying arbitrary residual statics to flatten arrivals to account for streamer curvature.

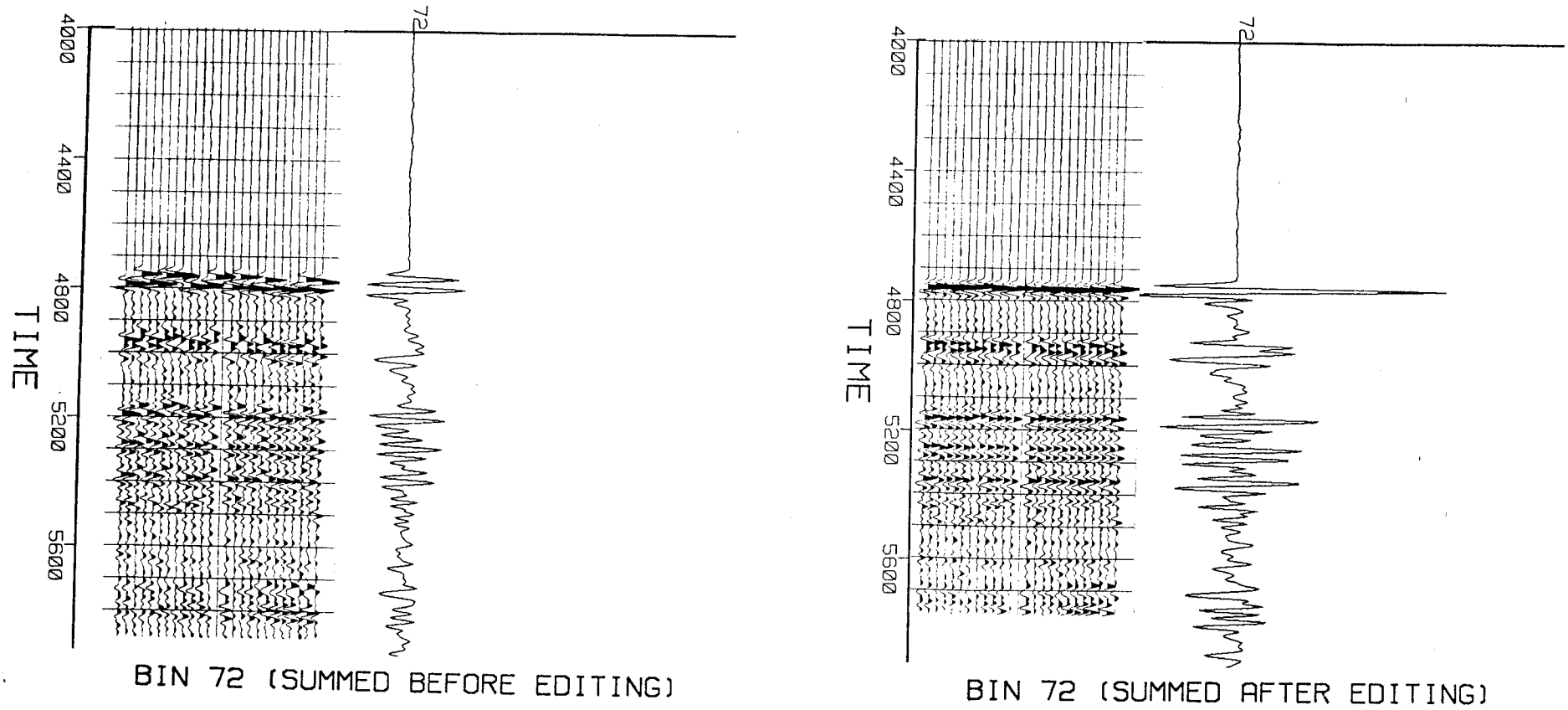

FIGURE 7e. Bin trace gather 3600 meters offset range, (Bin 72). Left is before application of static corrections to account for non-end fire shooting geometry and curvature of streamer as the ships passed. Right is after statics applied. Note markedly improved signal to noise ratio of the summed data trace shown to the right of each gather after statics applied.

can be attributed to the curvature in the streamer, which is common as the ships maneuver when they pass near the mid-point. This curvature can be accounted for by simply adding an arbitrary residual travel time static to each receiver channel to insure that the water bottom reflection wave train is indeed flat or isochronous (Figure 7d). The need to account for the precise shot-receiver channel range is demonstrated in Figure 7e. Without acoustic range corrections for streamer curvature and the non-end shooting aspect on the streamer (left) the signal-to-noise level resulting from bin summing is quite low compared to the bin sum after acoustic corrections (right).

3) Intermediate Offsets:

For calculating shot-receiver channel distances (offsets) for the ships' range interval beyond observation of direct and bottom reflected water waves across the streamer and before employment of the LORAN-C calculated ships' separation distances beyond the line of sight, the MINIRANGER radar system was used. Here the streamer was assumed to be trailing straight along the ships' track and the shot receiver channel distance was calculated by noting the respective antennae offset.

RESULTS

Plots of the travel time-offset range seismic record for each expanding spread profile (ESP 2, 3, 4, and 5) are shown in Figures 8, 9, 10, and 11, respectively. The multichannel seismic (MCS) profile collected along each ESP line is also shown (Figures 12, 13, 14 and 15). The approximate common mid-point (CMP) and the location of the offset interval for the plotted ESP data is shown by the arrows above the respective MCS profile accompanying each ESP line. Note that each ESP data trace is the result of summing several adjacent traces into the nearest 50 meter offset bin along the profile. Typically 3-6 traces were summed after applying an 8 km/sec reduction velocity static shift to account for the moveout for each trace's position within the bin width interval (+/- 25 meters).

Careful inspection of the MCS profiles over the offset range interval for each ESP plot (Figures 12, 13, 14, and 15) reveals the ESP experiments were indeed conducted in regions having a relatively simple, horizontally layered geologic structure. Only at the eastern end of ESP 4 do there appear to be significant, shallow diapir and fold structures which might complicate seismic arrivals from deeper crustal features. However, it should be noted that the maximum estimated dips here are still only about 5 degrees.

DATA ANALYSIS

Expanding spread profiles are particularily well-suited to acquire high signal to noise ratio seismic data over complex geologic structures with dips as large as 10 degrees and lateral velocity variations of 10% over a few km (Diebold and Stoffa, 1981). The symmetric ray path geometry of the upgoing and downgoing waves appears to compensate for small travel time delays in the seismic frequency band (5-50hz). Given the relatively simple structure encountered in these ESP experiments and the inherent high S/N ratio afforded by the dense spatial sampling and temporal resolution of multichannal ESP experiments means that relatively simple computer graphic techniques can be used to analysze the ESP results shown in Figures 8, 9, 10, and 11.

Travel Time Modeling:

The first technique employed was simple one-dimensional ray tracing. This was an iterative procedure in which we computed the first arrival time curves for the reflections from a model having horizontal uniform velocity layers using a hyperbolic normal moveout algorithm. These curves were then plotted and compared (superimposed) with the observed ESP seismic sections (Figures 8, 9, 10, and 11 left). Discrepencies between the observed data and the computed synthetic curves were noted and repeated adjustments were made in the velocity and thickness of the model's layers. The final reflection travel time curves of the model which appeared to best fit the observed seismic data for each ESP seismic section are shown at the right in Figures 8, 9, 10, and 11. The interval velocities of the layer model used to compute the synthetic travel time curves is shown at the left side between each curve and in Table 4. Note that several refraction arrivals are also observed in the seismic sections for ESP 3, 4, and 5 (Figures 9, 10, and 11, respectively). The refracted arrivals from a shallow sediment layer in ESP 3 (Figure 9) and the top of an allocthonous salt lense beneath ESP 4 are particularily distinctive (Figure 10). They can be traced back to near-normal incidence (zero offset) pre-critical reflections showing intercept times of about 3.8 and 2.8 seconds (two-way travel time), respectively. Also post-critical reflections for these events are clearly seen. A similar

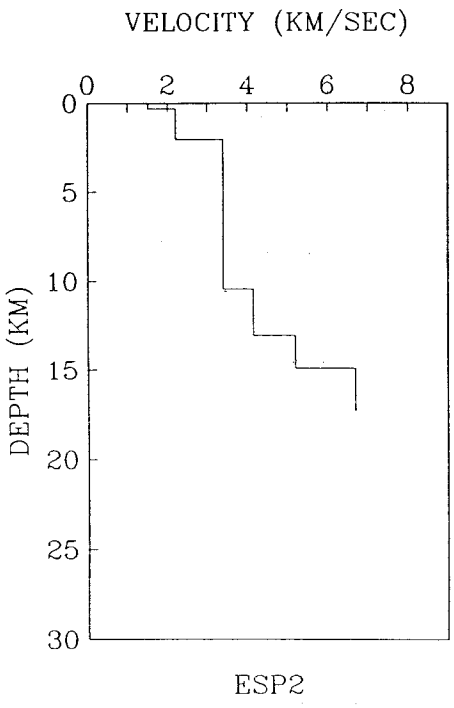

FIGURE 16. Velocity-depth profile derived from ray trace travel time modeling of ESP 2 (Fig. 8).

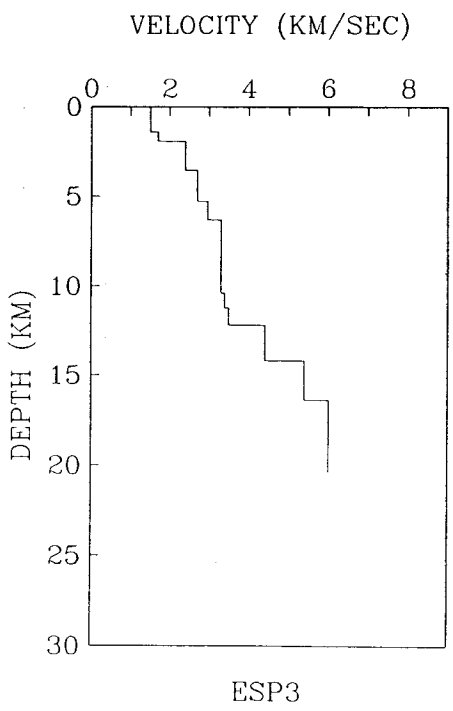

FIGURE 17. Velocity-depth profile derived from ray trace travel time modeling of ESP 3 (Fig. 9).

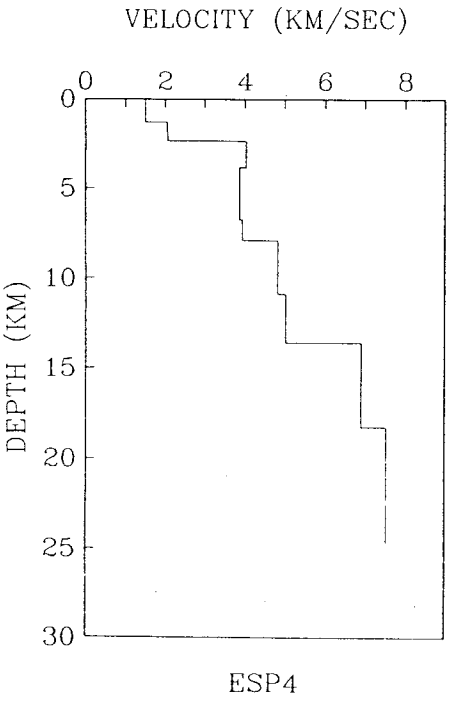

FIGURE 18. Velocity-depth profile derived from ray trace travel time modeling of ESP 4 (Fig. 10).

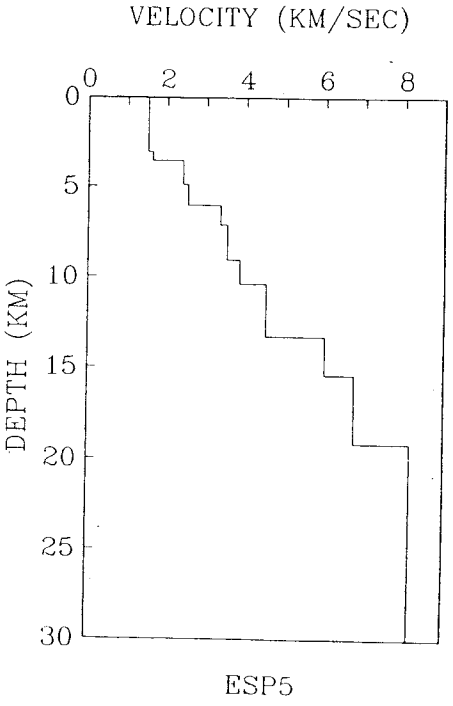

FIGURE 19. Velocity-depth profile derived from ray trace travel time modeling of ESP 5 (Fig. 11a,11b).

TABLE 4

Interval Velocity Models Derived from 1-D Synthetic Ray Tracing

ESP 2 TIME (SEC)	DEPTH (KM)	INTERVAL VELOCITY (KM/S)
0	0	
		1.510
.400	.302	
		2.200
1.985	2.045	
		3.387
6.950	10.453	
		4.150
8.200	13.047	
		5.200
8.900	14.867	
		6.700
9.600	17.212	

ESP 3 TIME (SEC)	DEPTH (KM)	INTERVAL VELOCITY (KM/S)
0	0	
		1.500
1.900	1.425	
		1.696
2.500	1.939	
		2.398
3.850	3.552	
		2.697
5.100	5.238	
		2.970
5.800	6.278	
		3.300
8.250	10.320	
		3.390
8.750	11.168	
		3.498
9.300	12.130	
		4.375
10.200	14.107	
		5.400
11.000	16.267	
		6.000
12.300	20.167	

ESP 4 TIME (SEC)	DEPTH (KM)	INTERVAL VELOCITY (KM/S)
0	0	
		1.500
1.736	1.302	
		2.042
2.750	2.337	
		4.020
3.500	3.845	
		3.850
5.010	6.752	
		3.925
5.600	7.909	
		4.800
6.850	10.909	
		5.000
7.950	13.659	
		6.900
9.300	18.317	
		7.500
11.000	24.692	

ESP 5 TIME (SEC)	DEPTH (KM)	INTERVAL VELOCITY (KM/S)
0	0	
		1.510
4.070	3.073	
		1.622
4.624	3.522	
		2.404
5.752	4.878	
		2.525
6.658	6.022	
		3.332
7.300	7.091	
		3.518
8.400	9.026	
		3.830
9.100	10.367	
		4.500
10.400	13.292	
		6.000
11.100	15.392	
		6.960
12.200	19.220	

refraction event with pre- and post-critical reflections can can be identified in the far offset traces of the ESP 5 seismic section (Figure 11). Although the pre-critical reflection here can not be traced completely back to near-normal incidence, the intercept time at normal incidence appears to be about 12.0 seconds (two-way travel time). Its apparent high velocity (8.1 km/sec) suggests that this refraction event is a mantle arrival. The velocity-depth profile derived from the 1-D ray tracing model for each ESP and the few observed refraction events is shown in Figures 16, 17, 18, and 19.

Tau-P Domain Slant Stacking and Direct Velocity Inversion:

The second technique used to analysze the ESP data was to transform the travel time-offset range (X-T) domain data to the intercept time-slowness ray parameter (Tau- P) domain using slant stacking techniques (Stoffa et al., 1981). The critical path of maximum coherence for the primary reflection as well as refraction arrivals was then visually estimated and inverted by simple integration (Tau-sum) to yield directly the velocity-depth profile (Diebold and Stoffa, 1981).

The Tau-P transformed plots of the ESP 2, 3, 4, and 5 seismic sections (Figures 8, 9, 10, and 11) are displayed in Figures 20, 21, 22, and 23, respectively. The interpreted critical path is also superimposed on each plot. Figures 24, 25, 26, and 27 show a comparison of the Tau-sum direct inversion velocity-depth profiles for each ESP line with the profiles derived from the 1-D ray trace models (Figures 16, 17, 18, and 19).

The velocity-depth profiles resulting from the above two analysis techniques show best agreement for ESP 5 (Figure 27). Significantly, it is here that the geologic structure might be expected to be more nearly horizontal and laterally homogeneous (Figure 15). Also, the high signal to noise ratio of the slant stacked Tau-P domain data set here as compared to the other ESP lines permitted an unambiguous interpretion of the critical path trajectory across the seismogram. For the other Tau-P transformed seismic sections the critical path determination was less constrained.

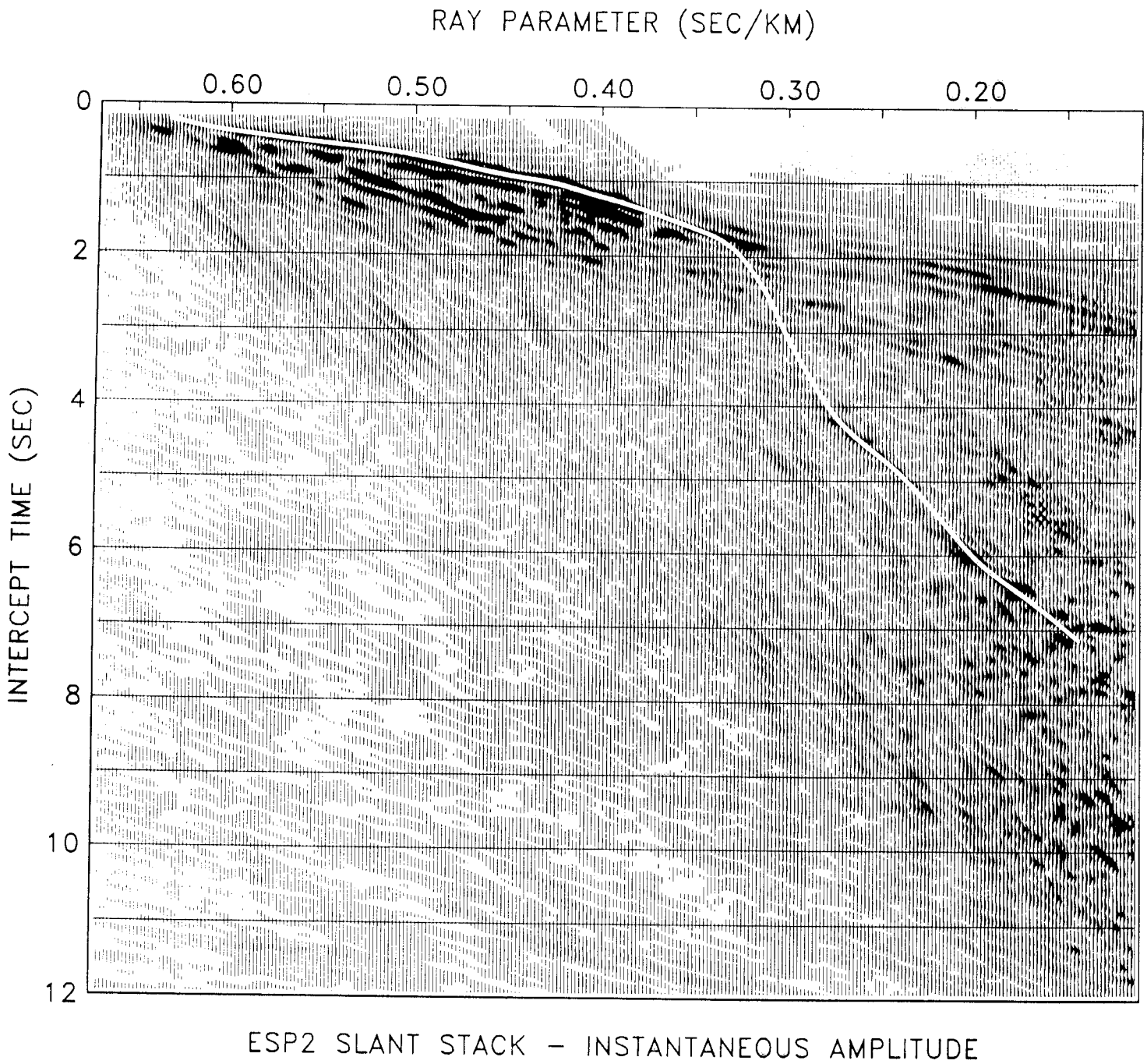

FIGURE 20. ESP 2. Slant-stacked, Tau-p transformation of X-T section with interpreted critical path (white line) superimposed. Data have been low pass filtered and Hilbert transformed to facilitate picking of the critical path.

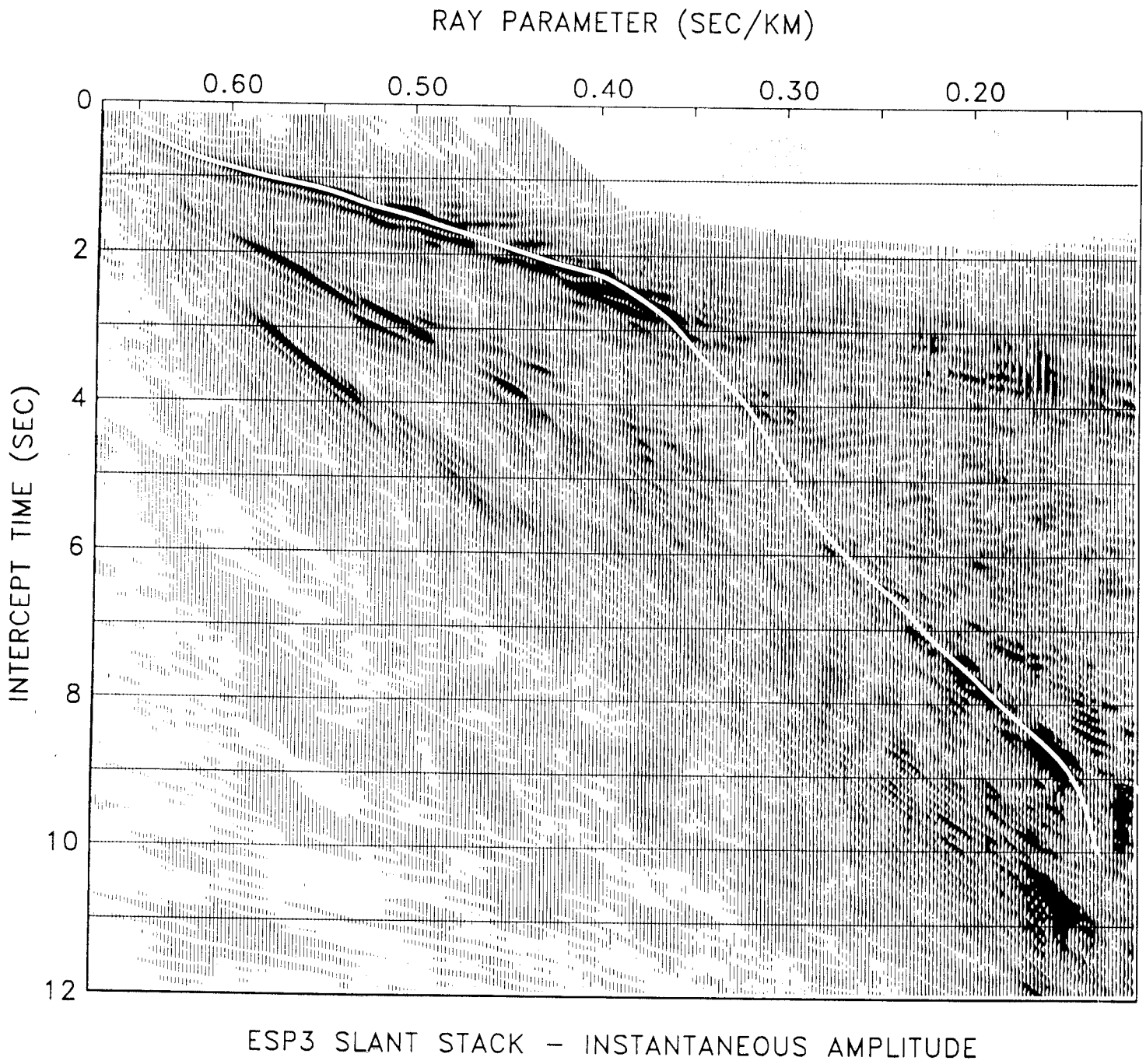

FIGURE 21. ESP 3. Slant-stacked, Tau-p transformation of X-T section with interpreted critical path (white line) superimposed. Data have been low pass filtered and Hilbert transformed to facilitate picking of the critical path.

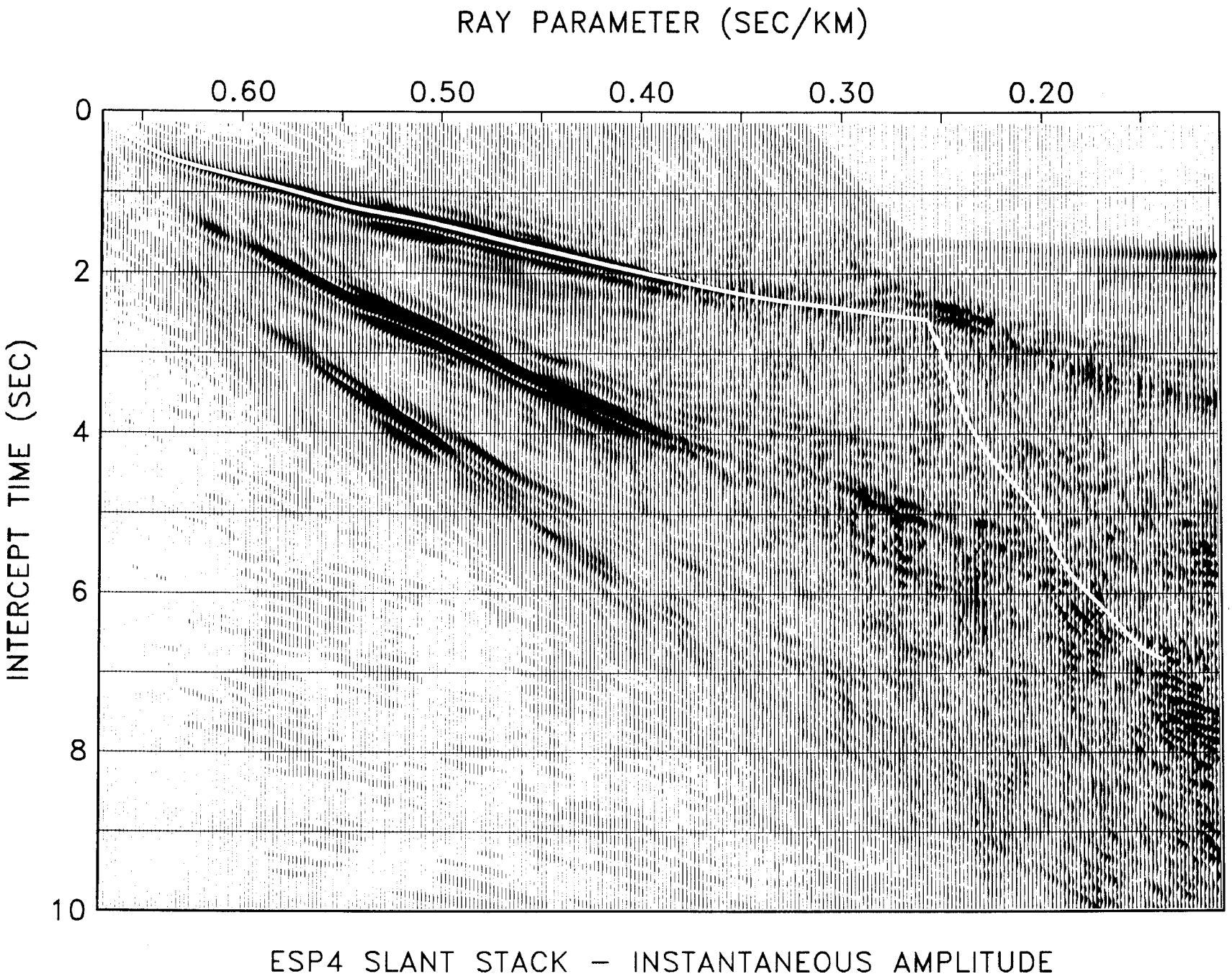

FIGURE 22. ESP 4. Slant-stacked, Tau-p transformation of X-T section with interpreted critical path (white line) superimposed. Data have been low pass filtered and Hilbert transformed to facilitate picking of the critical path.

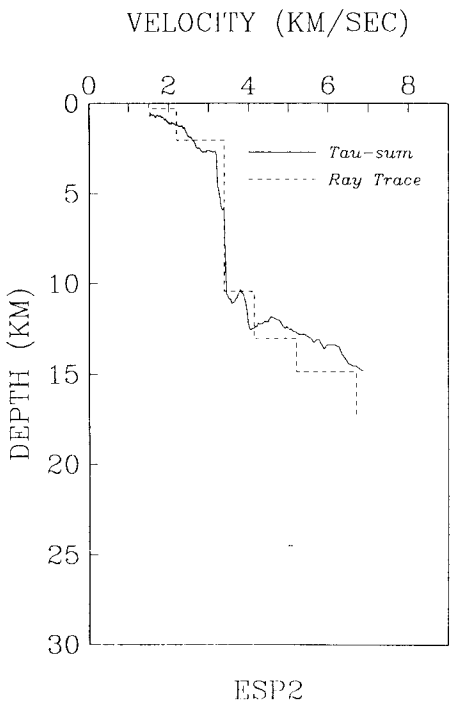

FIGURE 24. ESP 2. Comparison of velocity-depth profile derived from direct inversion of Tau-p critical path with ray trace travel time derived profiles.

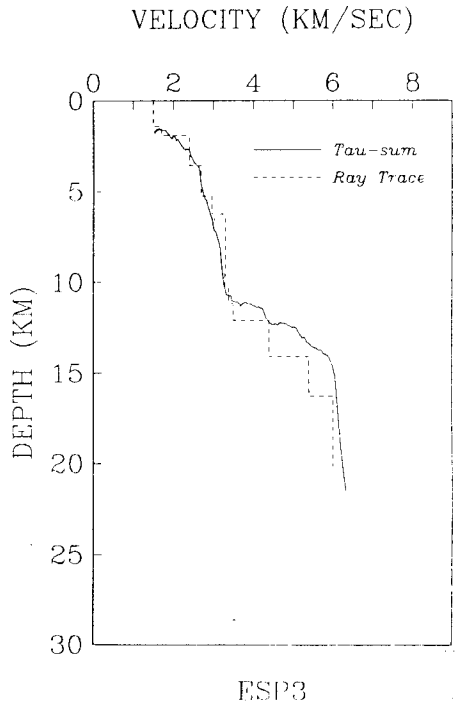

FIGURE 25. ESP 3. Comparison of velocity-depth profile derived from direct inversion of Tau-p critical path with ray trace travel time derived profiles.

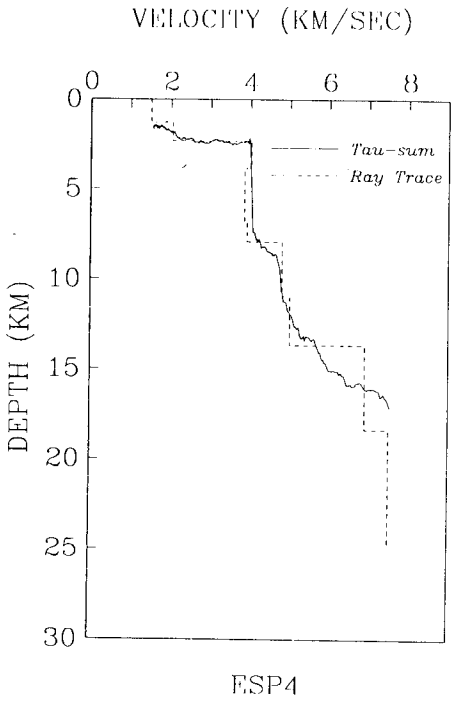

FIGURE 26. ESP 4. Comparison of velocity-depth profile derived from direct inversion of Tau-p critical path with ray trace travel time derived profiles.

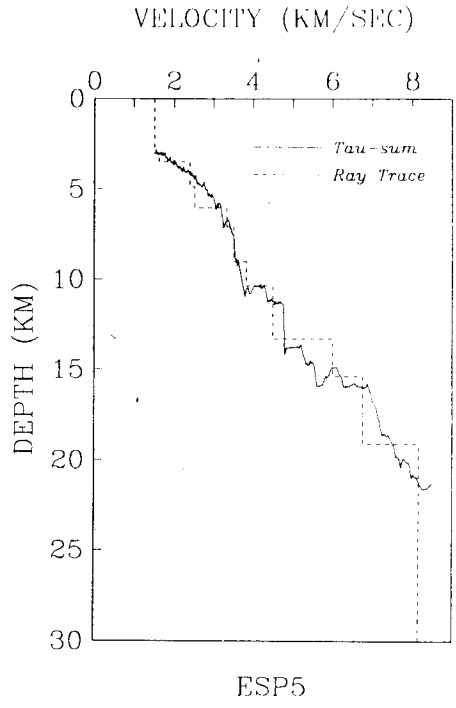

FIGURE 27. ESP 5. Comparison of velocity-depth profile derived from direct inversion of Tau-p critical path with ray trace travel time derived profiles.

GEOLOGIC INTERPRETATION

The ESP and MCS seismic results presented in this report have provided information useful for interpretation of the detailed seismic stratigraphy of the Texas-Louisiana continental margin as well as the deep crustal stucture beneath the region.

Seismic Stratigraphy:

To demonstrate the use of the ESP results for interpreting the seismic stratigrapy of conventional multichannel seismic (MCS) profiles, we have juxaposed the portions of deep penetration MCS profiles shot in the vicinity of the ESP4 and 5 mid-points with their respective ESP seismic section (Figures 28 and 29). Note that hyperbolic normal moveout has been applied to the ESP seismic sections using the velocity-time functions shown in Figures 18, and 19.

Careful correlation of the seismic horizons seen in the MCS profiles with the NMO corrected arrivals of the ESP 5 section reveals that precise interval velocities can be assigned to each of the stratigraphic units identified in the MCS profiles (Figures 15 and 29). This correlation allows extension of the stratigraphy of the deep Gulf of Mexico basin (Buffler, et al., 1978) across the continental rise/slope landward of the Sigsbee Escarpment. Such velocity information when combined with available MCS profiles which cross the Sigsbee Escarpment (Figure 30) provide confident identification of the deep primary reflectors commonly seen beneath the detached salt lenses on the continental rise/slope. Also, an estimate for the base of the salt lenses here can be made which suggests a thickness of about 1 second or less (two-way travel time) or about 2 km, assuming a 4.0 km/sec compressed wave velocity for salt here (Figures 10 and 18).

Comparison of the NMO corrected, ESP section with its respective MCS profile is also useful for distinguishing primary reflection horizons from multiple reverberations (Figure 29). For example, the strong reflection seen at about 0.5 seconds beneath the Moho reflection identified in the MCS profile along ESP 5 is clearly a multiple since it correlates with an ESP arrival which still shows considerable residual moveout (downward curvature) after NMO

correction. In contrast, several deep reflectors including strong events beneath the the salt lenses in ESP 4 appear to be primary reflections (i.e., top of Campeche and MCU formations) by virtue of their correlation with nearly horizontal events in the respective NMO corrected ESP sections (ESP 4, Figure 28).

Deep Crustal Structure:

The ESP sections also provide data from reflection and refraction events emanatating from structure well below the reflection horizons seen in conventional MCS profiles. For example, ESP 2 at the Shelf edge, ESP 3 over the Caranchua basin and ESP 4 over the detached salt lense on the slope show several primary reflections with normal incidence times greater than 8.0 seconds (Figures 8, 9 and 10). Typical MCS profiles are generally limited to about 6.0-8.0 seconds penetration here. Also, beneath ESP 5 several deep reflection events (Figure 29) as well as a mantle refraction/reflection arrivals (Figure 11) have been observed which emanate from well below the MCU reflector at 9.0 seconds, heretofor the deepest MCS sedimentary horizon generally seen in the deep Gulf of Mexico.

To illustrate the deep structural information obtained from the ESP observations, we have constructed a composite gravity and velocity-depth cross-section along the Gulf of Mexico Transect (94 degrees West Longitude) shown in Figure 31. This transect line was previously established by Pilger and Angelich (1984). The ESP velocity-depth profiles shown in Figures 16, 17, 18, and 19 have been projected on to this composite transect. Also, the ocean bottom seismometer velocity-depth profile results reported in the accompanying Part B report by Ebeniro et al., 1986, are projected on the Gulf of Mexico Transect line. It is clear from both the ESP and OBS velocity-depth profiles that transitional, continental crust-type material extends well out beneath the slope and rise. Also, there appears to be a thickened section of ocean crustal material beneath the Sigsbee Escrapment (ESP 4). However it should be noted that this oceanic-like section is separated from the transitional continental crust at the shelf edge by a thinned oceanic-like section beneath the Caranchua basin (ESP 3). In fact, the OBS refraction results indicate a shallow mantle here. Unfortunately, the ESP observations

did not detect mantle refractions here. The deepest observed reflection did provide an interval velocity of about 6.9 km/sec at a depth of about 20 km which is characteristic of the materials lying just above the mantle in this region (Ewing et al., 1960; Antoine and Ewing 1963).

CONCLUSIONS

Expanding spread profile (ESP) experiments in the northern Gulf of Mexico have provided new information about the detailed seismic stratigraphy as well as the deep crustal structure beneath the Texas-Louisiana continental margin. Specifically:

1) The deep structure beneath the rise and slope is marked by large variation in the velocity and depth of the basement rocks underlying the thick sedimentary section. Oceanic type basement rocks beneath the Caranchua basin appear to separate the thick, transitional section of continental crust at the shelf edge from a thickened section of transitional oceanic crust near the Sigsbee Escarpment. On the rise near-normal thickness and velocity oceanic crust is observed with the Moho (8.1 km/sec) at about 20 km depth.

2) Major seismic stratigraphic units recognized in the deep Gulf of Mexico (i.e., Campeche formation and Middle Cretaceous Unconformity) can be traced landward of the Sigsbee escarpment beneath the salt lenses on the slope.

3) The allocthonous salt lenses, themsleves, are relatively thin structures with their maximum thickness estimated to be less than 2 km.

Acknowledgements. This project was conceived by a group of scientists at the Institute for Geophysics led by Arthur E. Maxwell, and other scientists at the U.S. Geological Survey, Woods Hole. Art Maxwell's field participation and encouragement throughout this study is gratefully acknowledged. Charles Denham and Mark Wiederspahn developed the computer programs for calculating the shot receiver offset distance and trace header editing procedures. Paul Stoffa reviewed the manuscripts. Captain Bruce H. Collins of R/V *Fred H. Moore* and his crew were instrumental in making this experiment successful. Kenneth H. Griffiths, Eric Rosencrantz, Archie Roberts, Douglas McCowan, Charles Windisch, Debbie Denino, William Behrens, John Crowe, John Parks, George W. Pearcy, Stirling Gilfillan, and Oscar Febres-Cordero were responsible for the many ship-related operations including electronics, mechanical work, navigation, data acquisition and communication. Also, J. Grow, R.

Mattick, A. Trehu, T. O'Brien and T. Edgar, all with the USGS participated in the field study. N. Zilhman of the USGS processed the *Gyre* single-ship seismic data. The 1-D synthetic ray tracing program used in this study was developed by Tracy Stark. K. Moser typed the manuscript.

REFERENCES

Antoine, J. and J. Ewing, Seismic refraction measurements on the margins of the Gulf of Mexico, *J. Geophys. Res., 68,* 1975-1996, 1963.

Buffler, R. T., J. L. Worzel and J.S. Watkins, Deformation and origin of the Sigsbee scarp - lower continental slope, northern Gulf of Mexico, *Offshore Tech. Conf. 3,* OTC 3217, 1425-1433, 1978.

Diebold, J. B. and P. L. Stoffa, The travel time equation, tau-p mapping and inversion of common midpoint data, *Geophysics, 46,* 238-354, 1981.

Ebeniro, Joseph O., D. S. Sawyer, Y. Nakamura, F. J. Shaub and W. P. O'Brien, Deep Structure of the shelf and slope of the northern Gulf of Mexico; Part B: An ocean-bottom seismograph-airgun experiment, Univ. of Texas, Institute for Geophysics Technical Report 41, 37 pp. 1985.

Ewing, J., J. Antoine and M. Ewing, Geophysical measurements in the western Caribbean Sea and in the Gulf of Mexico, *J. Geophys. Res., 65,* 4087-4126, 1960.

Pilger, R. H., Jr. and M. T. Angelich, Gravity Anomalies, in *Ocean Margin Drilling Program Regional Atlas Series, Atlas 6, Gulf of Mexico,* edited by R. T. Buffler, S. D. Locker, W. R. Bryant, S. A. Hall and R. H. Pilger, Jr., Sheet 2, Marine Science International, Woods Hole, 1984.

Stoffa, P. L. P. Buhl, J. B. Diebold, and F. Wenzel, Direct mapping of seismic data to the domain of intercept time and ray parameter - A plane wave decomposition, *Geophysics, 46,* 255-267, 1981.

Stoffa, P. L., and P. Buhl, Two-ship multichannel seismic experiments for deep crustal studies: Expanded spread and constant offset profiles, *Journal of Geophysical Research,* Vol. 84, no. B13, p. 7645-7660, 1979.

APPENDIX TABLES

Seismic line descriptions and sonobuoy station locations

R/V Fred Moore (Cruises 20-1 and 20-2) and R/V Gyre (Cruise 83-14)

Northern Gulf of Mexico
(Texas-Louisiana Continental Margin)

TABLE A

GULF OF MEXICO TRANSECT
CRUISE FM 20-01

LINE	START TIME	END TIME	START DFS/SHOT	END DFS/SHOT	START/END FIELD TAPE#	START LAT	START LON	END LAT	END LON	LORAN/C TIME DELAY	SHOOT/REC SHIPS INTERVAL	LINE TYPE # TRACES
GMT-1	0505/12NOV	1812/12NOV	0001/0001	1744/1744	0112/0122					<NORTHSTAR	G/G 30/15	ESP1/ PRESHOOT 24
GMT-2	0300/14NOV	1208/14NOV	0001/0001	1097/1096	200001/200013	27 47.15	95 11.99	27 49.90	94 19.47		M/M 30/15	ESP2/ PRESHOOT 48
						11137.2-	24971.2-	11181.1-	25509.2-	<NORTHSTAR		
GMT-3A	2015/14NOV	0115/15NOV	0001/0001	0282/0299	200014/200021	27 49.85	94 20.64	27 48.25	94 43.84		-/M -/40	ESP2A 48
						11179.9-	25499.8-	11159.4-	25258.2-	<NORTHSTAR		
						11179.93	25499.63	11159.00	25255.32	< L/C 404		
GMT-3A	2015/14NOV	0122/15NOV	0001/0001	0308/0308	0123/0124	27 47.00	95 09.89	27 48.47	94 45.86		G/G 60/15	ESP2A 24
										<NORTHSTAR		
						11138.98	24991.18	11157.13	25238.90	< L/C 404		
GMT-3B	0122/15NOV	0209/15NOV	0286/0307	0333/0355	200022/200022	27 48.37	94 44.18	27 48.13	94 47.57		M/M 60/15	ESP2B 48
						11158.9-	25255.3-	11156.1-	25219.9-	<NORTHSTAR		
						11159.00	25255.32	11156.18	25219.74	< L/C 404		
GMT-3B	0146/15NOV	0213/15NOV	0311/0311	0338/0338	0125/0125	27 49.56	94 43.82	27 50.15	94 41.63		-/G -/40	ESP2B 24
										<NORTHSTAR		
						11157.20	25264.82	11158.26	25289.72	< L/C 404		
GMT-3C	0601/15NOV	1045/15NOV	0335/0640	0619/0959	200023/200026	27 48.34	94 45.41	27 46.68	95 12.91		M/M 60/15	ESP2C 48
						11137.8-	25242.9-	11137.1-	24959.5-	<NORTHSTAR		
						11157.74	25242.84	11137.15	24959.27	< L/C 404		
GMT-3C	0601/15NOV	1045/15NOV	0341/0341	0652/0652	0126/0131	27 47.43	94 46.49	27 49.82	94 19.56		-/G -/40	ESP2C 24
										<NORHTSTAR		
						11158.26	25227.46	11181.07	25510.62	< L/C 404		
GMT-4	1100/15NOV	1900/15NOV	0636/0983	1115/1528	200027/200032	27 45.87	95 13.85	27 05.04	95 21.24		M/M 60/15	CDP TIELINE 48
						11137.6-	24946.1-	11193.1-	24678.8-	<NORTHSTAR		
GMT-5	0450/16NOV	1021/16NOV	0010/0010	0341/0341	0132/0137	26 50.99	94 27.01	26 59.81	94 53.85		-/G 0/40	ESP3 24
										<NORTHSTAR		
						11279.57	25186.69	11230.23	24941.36	< L/C 404		
GMT-5	0450/16NOV	1635/16NOV	0015/0015	0714/0719	200033/200041	27 03.93	95 15.86	26 48.27	94 18.05		M/M 60/15	ESP3-CDP PRE&SIMUL SHOOT 48
						11200.1-	24730.0-	11297.3-	25269.7-	<NORTHSTAR		
						11200.14	24730.17	11297.22	25269.63	< L/C 404		
GMT-6	1130/16NOV	1642/16NOV	0001/0001	0289/0289	0139/0140	26 58.08	94 52.94	26 51.66	94 29.33		-/G	XOP

						11234.20 24944.20 11275.30 25166.14< L/C 404	<NORTHSTAR	-/20	24
GMT-7	1643/16NOV	1946/16NOV	0715/0727	0898/0910	200041/200043	26 48.14 94 17.28 26 46.70 94 00.17 11298.7- 25277.2- 11328.0- 25448.5-<NORTHSTAR		M/M 30/15	CDP TIELINE 48
GMT-7	1652/16NOV	1945/16NOV	0002/0002	0174/0174	0141/0142	26 51.48 94 28.53 26 49.62 94 13.52 11276.59 25172.73 11301.51 25321.15< L/C 404	<NORTHSTAR	-/G -/20	XDP 24
GMT-8X	0940/17NOV	1234/17NOV	0001/0001	0402/0463	200044/200048	26 34.24 93 47.91 26 45.66 93 34.19 11373.3- 25532.3- 11375.5- 25711.4-<NORTHSTAR 11373.26 25532.86 11375.63 25711.56< L/C 404		-/M -/20	XDP 48
GMT-9	0632/17NOV	0709/17NOV	0007/0007	0095/0095	0143/0143		<NORTHSTAR	G/G 20/15	ESP4 CDP PRESHOOT 24
GMT-9A	0940/17NOV	1318/17NOV	0001/0001	0500/0500	0144/0146	26 30.36 93 52.33 26 39.71 93 41.13 11372.99 25474.69 11374.69 25619.96< L/C 404	<NORTHSTAR	G/G 20/15	ESP4 CDP PRESHOOT 24
GMT-9	1340/17NOV	1917/17NOV	0406/0610	0738/0948	200049/200058	26 44.27 93 35.35 26 27.08 93 56.09 11376.2- 25694.7- 11372.8- 25425.9-<NORTHSTAR 11376.20 25694.81 11372.80 25426.07< L/C 404		-/M -/40	ESP4 48
ESP-4	1334/17NOV	1917/17NOV			0147/0148	26 40.59 93 40.20 26 58.94 93 18.92 11374.61 25632.50 11376.99 25916.13< L/C 404	<NORTHSTAR	G/G 60/15	ESP4-CDP SIMUL- SHOOT 24
GMT-10A	1933/17NOV	2110/17NOV	0749/0970	1039/1260	200059/200062	26 26.39 93 56.93 26 22.59 94 00.03 11372.6- 25415.4- 11374.5- 25372.2-<NORTHSTAR		M/M 20/15	CDP TIELINE 48
GMT-10B	2110/17NOV	0300/18NOV	1040/1261	1741/1962	200062/200070	26 22.58 94 00.03 26 01.10 93 59.67 11374.5- 25372.1- 11415.3- 25317.2-<NORTHSTAR		M/M 30/15	CDP TIELINE 48
GMT-11	0301/18NOV	1230/18NOV	1742/1963	2880/3101	200070/200084	26 01.09 93 59.63 26 00.01 93 05.34 11415.3- 25317.5- 11528.4- 25858.3-<NORTHSTAR		M/M 30/15	ESP5-CDP PRESHOOT 48
GMT-12A	1514/18NOV	1727/18NOV	3000/3321	3133/3454	200085/200088	25 59.91 93 07.69 25 59.94 93 18.63 11523.1- 25834.7- 11498.7- 25725.8-<NORTHSTAR 11523.19 25834.78 11498.72 25725.80< L/C 404		-/M -/40	ESP5A 48
GMT-12A	1514/18NOV	1727/18NOV			0149/0150	26 00.02 93 54.66 26 00.02 93 43.75 11426.29 25364.79 11446.94 25474.48< L/C 404	<NORTHSTAR	G/G 60/15	ESP5A-CDP SIMUL- SHOOT 24
GMT-12B	2010/18NOV	0000/19NOV	3296/3617	3526/3847	200090/200097	26 00.31 93 29.37 26 00.17 93 49.02 11475.0- 25618.5- 11436.6- 25422.0-<NORTHSTAR 11474.92 25617.70 11436.70 25421.15< L/C 404		-/M -/40	ESP5B 48

GMT-12B 2010/18NOV 0000/19NOV	25 57.86 93 32.85 25 59.98 93 15.61 <NORTHSTAR 11472.72 25578.05 11505.24 25755.99< L/C 404	G/G 60/15	ESP5B-CDP SIMUL- SHOOT 24
GMT-13 0547/19NOV 1400/19NOV 0004/0003 0985/0989 200098/200112	26 03.71 93 33.83 26 41.93 93 45.38 11459.5- 25583.9- 11362.6- 25583.9-<NORTHSTAR 11459.59 25583.90 11362.61 25583.99< L/C 404	M/M 60/20 G/M 60/20	CDP 48
GMT-13 0543/19NOV 1400/19NOV	26 09.96 93 35.97 26 47.45 93 47.62 <NORTHSTAR 11443.25 25579.86 11347.56 25580.08< L/C 404	G/G 60/20 M/G 60/20	CDP 24
GMT-14 1447/19NOV 1529/19NOV 0987/1068 1071/1152 200112/200113	26 45.65 93 46.77 26 47.19 93 48.99 11352.6- 25582.5- 11345.7- 25565.2-<NORTHSTAR	M/M 60/15	CDP 48
GMT-15 1529/19NOV 0613/20NOV	26 47.19 93 48.99 28 14.89 94 16.92 11345.7- 25565.2- 11138.9- 25660.8-<NORTHSTAR	M/M	3.5KHZ ONLY

GULF OF MEXICO TRANSECT
ESP AVERAGE MIDPOINTS

LINE	LATITUDE	LONGITUDE
ESP2	27 48.31	-94 46.20
ESP3	26 58.35	-94 51.48
ESP4	26 43.21	-93 37.75
ESP5	26 00.00	-93 31.47

TABLE B

GULF OF MEXICO TRANSECT
SONOBUOY STATIONS
CRUISE FM 20-01

SONOBUOY STATION#	LINE #	START TIME	START LAT	START LONG	START DFS/SP#	START TAPE#	LINE TYP	RECORD DFS	CHANNELS DMUXR	SB CHAN/TYPE	WATER TEMP/VEL	RECORD INTERVAL	COMMENTS
1	GMT-2	0329/14NOV	27 47.37	95 09.14	0059/0059	200001	ESP2-CDP PRESHOOT	53/54	60/61	30/41A		0/15	GOOD SB/NO RF XMIT AFTER 1.5 HOURS
2	GMT-2	0458/14NOV	27 47.55	95 00.56	0237/0237	200003	ESP2-CDP PRESHOOT	53/54	60/61	29/41A		0/15	GOOD SB, 3 HOURS RF XMIT
3	GMT-2	0715/14NOV	27 48.58	94 47.16	0511/0511	200007	ESP2-CDP PRESHOOT	53/54	60/61	8/41		0/15	NO XMIT
4	GMT-2	0805/14NOV	27 48.64	94 42.50	0611/0611	200008	ESP2-CDP PRESHOOT	53/54	60/61	6/41		0/15	NOISY RF XMIT AFTER 40 MINS.
5	GMT-2	0908/14NOV	27 48.74	94 36.56	0737/0737	200009	ESP2-CDP PRESHOOT	53/54	60/61	30/41A		0/15	GOOD SB, 3HOURS RF XMIT
6	GMT-5	0606/16NOV	27 02.37	95 09.08	/0091	200034	ESP3-CDP SIMUL-SHOOT	53/54	60/61	30/41A		0/15	GOOD SB, 3 HOURS RF XMIT
7	GMT-5	0906/16NOV	26 58.70	94 55.31	0420/0272	200036	ESP3-CDP SIMUL-SHOOT	53/54	60/61	14/41		0/15	NO RF XMIT
8	GMT-5	0917/16NOV	26 58.40	94 54.42	0443/0283	200036	ESP3-CDP SIMUL-SHOOT	53/54	60/61	4/41		0/15	NO RF XMIT
9	GMT-5	0930/16NOV	26 58.18	94 53.33	0450/0296	200036	ESP3-CDP SIMUL-SHOOT	53/54	60/61	30/41A		0/15	GOOD SB, 3 HOURS RF XMIT
10	GMT-10B	2120/17NOV	26 22.00	94 00.00	1070/1291	200062	CDP TIE LINE	53/54	60/61	29/41A		0/15	GOOD SB, +3 HOURS RF XMIT
11	GMT-10B	0031/18NOV	26 11.66	94 00.09	1442/	200067	CDP TIE LINE	53/54	60/61	30/41A		0/15	GOOD SB, +3 HOURS RF XMIT
12	GMT-11	0401/18NOV	26 00.15	93 55.71	1862/2083	200072	ESP5-CDP PRESHOOT	53/54	60/61	6/41		0/15	RF XMIT, BUT NO PHONE
13	GMT-11	0414/18NOV	26 00.13	93 54.60	1888/2109	200072	ESP5-CDP PRESHOOT	53/54	60/61	29/41A		0/15	STREAMER FOULED NOISY
14	GMT-11	0444/18NOV	26 00.93	93 51.93	1949/2170	200072	ESP5-CDP PRESHOOT	53/54	60/61	30/41A		0/15	STREAMER FOULED NOISY

15	GMT-11	0507/18NOV	26 00.75	93 49.80	1995/2216	200073	ESP5-CDP PRESHOOT	53/54	60/61	29/41A	0/15	GOOD SB, 3 HOURS RF XMIT
16	GMT-11	0826/18NOV	26 00.06	93 30.54	/2614	200078	ESP5-CDP PRESHOOT	53/54	60/61	8/41	0/15	NO RF XMIT AFTER 15 MINS.
17	GMT-11	0846/18NOV	25 59.97	93 28.44		200078	ESP5-CDP PRESHOOT	53/54	60/61	30/41A	0/15	GOOD SB, 3 HOURS RF XMIT
18	GMT-13	0452/19NOV	26 08.44	93 35.13	0202/0134	200099	COP3	53/54	60/61	4/41	0/20	GOOD SB, 13 HOURS RF XMIT
19	GMT-13	1022/19NOV	26 23.29	93 40.07	0550/0554	200106	COP3	53/54	60/61	30/41A	0/20	GOOD SB, 3 HOURS RF XMIT

TABLE C

GULF OF MEXICO TRANSECT
SONOBUOY STATIONS
CRUISE FM 20-02

SONOBUOY STATION#	LINE #	START TIME	START LAT	START LONG	START DFS/SP#	START TAPE#	LINE TYP	RECORD DFS	CHANNELS DMUXR	SB CHAN/TYPE	WATER TEMP/VEL	RECORD INTERVAL	COMMENTS
1	OBS-4	1511/28NOV	26 30.54	93 51.05	0143/0143	202001	OBS/ESP-4	53/54	06/07	30/41A		0/15	GOOD SB 3 HRS RF XMIT
2	OBS-4	1837/28NOV	26 43.50	93 37.03	0555/0555	202002	OBS/ESP-4	53/54	06/07	30/41A		0/15	GOOD SB, 3 HRS RF XMIT
3	OBS-5	0015/30NOV	25 59.05	93 54.25	0031/0030	202004	OBS/ESP-5	53/54	06/07	30/41A		0/15	GOOD SB, 3 HRS RF XMIT
4	OBS-5	0311/30NOV	25 59.74	93 37.94	0383/0382	202004	OBS/ESP-5	53/54	06/07	30/41A		0/15	GOOD SB, 3 HRS RF XMIT
5	OBS-5	0711/30NOV	25 59.60	93 15.95	0863/0862	202005	OBS/ESP-5	53/54	06/07	30/41A		0/15	GOOD SB, 3 HRS RF XMIT
6	OBS-3	1414/01DEC	27 02.29	95 10.20	0029/0029	202007	OBS/ESP-3	53/54	06/07	30/41A		0/15	GOOD SB, 3 HRS RF XMIT
7	SONOBUOY DID NOT OPERATE, NO RF XMIT												
8	SONOBUOY DID NOT OPERATE, NO RF XMIT												
9	OBS-3	1710/01DEC	26 58.19	94 54.60	0381/0380	202007	OBS/ESP-3	53/54	06/07	30/41A		0/15	GOOD SB, 3 HRS RF XMIT
10	OBS-3	1852/01DEC	26 55.76	94 45.45	0585/0584	202008	OBS/ESP-3	53/54	06/07	30/41A		0/15	GOOD SB, 3 HRS RF XMIT
11	OBS-2	0006/03DEC	27 49.54	94 22.84	0013/0013	202010	OBS/ESP-2	53/54	06/07	30/41A		0/15	GOOD SB, 3 HRS RF XMIT
12	OBS-2	0243/03DEC	27 48.81	94 38.04	0327/0326	202011	OBS/ESP-2	53/54	06/07	30/41A		0/15	GOOD SB, 3 HRS RF XMIT
13	OBS-2	0551/03DEC	27 47.69	94 56.21	0703/0702	202011	OBS/ESP-2	53/54	06/07	30/41A		0/15	GOOD SB, 3 HRS RF XMIT